



Invited Review

## Recent advances in metals and metal oxides as catalysts for vanadium redox flow battery: Properties, structures, and perspectives



Yanrong Lv<sup>a</sup>, Chao Han<sup>a</sup>, Ye Zhu<sup>a</sup>, Tianao Zhang<sup>a</sup>, Shuo Yao<sup>a</sup>, Zhangxing He<sup>a,b,\*</sup>, Lei Dai<sup>a,b,\*</sup>, Ling Wang<sup>a,b,\*</sup>

<sup>a</sup> School of Chemical Engineering, North China University of Science and Technology, Tangshan 063009, China

<sup>b</sup> Hebei Province Key Laboratory of Photocatalytic and Electrocatalytic Materials for Environment, North China University of Science and Technology, Tangshan 063009, China

ARTICLE INFO

Article history:

Received 23 July 2020

Received in revised form

18 September 2020

Accepted 27 September 2020

Available online 2 November 2020

Keywords:

Energy storage

Vanadium redox flow battery

Carbon-based material

Metal oxide

Metal

Electrocatalyst

ABSTRACT

Vanadium redox flow battery (VRFB) is a kind of battery with wide application prospect. Electrode material is one of the key components of VRFB, and its stability directly affects the performance of battery. Among all kinds of electrode materials, carbon-based material has the best comprehensive properties. However, carbon-based electrodes still have disadvantages such as poor hydrophilicity and low electrochemical activity which need to be improved. One of the effective ways to improve the performance of electrode is to modify carbon-based material with metals and metal oxides. The metal catalysts have excellent electrical conductivity and high catalytic activity. The metal oxide catalysts have the advantages of low cost, wide variety and strong oxidizing properties. This work introduced the application of metal and metal oxide modified electrodes in VRFB in recent years, classified the catalysts, studied their catalytic performance and mechanism. The metal catalysts were reviewed from precious metals and base metals. The metal oxide catalysts were classified and discussed according to the similar properties of the same group elements. This work compared different modification methods, summarized the research progress of metal and metal oxide modification, and proposes the future development direction of electrodes and catalysts.

© 2021 Published by Elsevier Ltd on behalf of The editorial office of Journal of Materials Science & Technology.

Contents

1. Introduction.....	97
2. Metal electrocatalysts.....	97
2.1. Precious metals.....	97
2.2. Base metals.....	98
3. Metal oxides electrocatalysts.....	99
3.1. Transition metal oxides electrocatalysts.....	99
3.1.1. IIIB group metal .....	99
3.1.2. IVB group metal .....	100
3.1.3. VB group metal.....	101
3.1.4. VIB group metal .....	102
3.1.5. VIIIB group metal .....	103
3.1.6. VIII group metal .....	104
3.2. Main group metal oxides: IVA group metal .....	105

\* Corresponding authors at: School of Chemical Engineering, North China University of Science and Technology, Tangshan 063009, China.

E-mail addresses: [zxhe@ncst.edu.cn](mailto:zxhe@ncst.edu.cn) (Z. He), [dailei.b@163.com](mailto:dailei.b@163.com) (L. Dai), [tswling@126.com](mailto:tswling@126.com) (L. Wang).

4. Conclusion and perspectives .....	106
Declaration of Competing Interest .....	107
Acknowledgements .....	107
Appendix A. Supplementary data.....	108
References .....	108

## 1. Introduction

With the rapid development of socio-economic and technological levels, a series of energy and environmental issues have also emerged [1–5]. The conventional energy is increasingly exposed its limitations, making it unable to meet the needs of public, and adding a burden of environment [6–9]. A lot of greenhouse gas emissions lead to climate warming [10]. Climate change has a great impact on human life [11,12]. Developing clean energy and reducing greenhouse gas emissions have become the key to solve problem [13–17]. Using renewable clean energy instead of traditional fossil fuel can reduce greenhouse gas emissions and protect environment. Renewable clean energy such as solar energy and wind energy has advantages of environmentally friendliness and inexhaustible supply. However, the production of clean energy depends on weather, making it impossible to provide continuous power [18,19]. Unstable electric energy is directly introduced into power grid, which causes serious damage to the power grid. The renewable clean energy needs to be converted into energy which can be stored and controlled. And then renewable clean energy can be introduced into power grid. Hence, in order to meet the needs of production and life, researchers have paid more attention to the development of energy storage and conversion technology [20–24].

Vanadium redox flow battery (VRFB) as an efficient energy storage device, has advantages of high reversibility, long life and fast response [25–29]. Fig. 1 shows the structure diagram of VRFB. As key component of VRFB, electrode provides reaction sites for vanadium ion, but does not involve in reaction. During the reaction, electrode material is always in a strongly acidic and oxidizing working environment. This requires that electrode material should have characteristics such as acid resistance, oxidation resistance and strong mechanical properties [30–32]. Electrode material can be divided into carbon-based, metal and polymer composite materials. Carbon-based materials have the characteristics of high acid resistance, strong electrical conductivity, large specific surface area and low cost, which has been widely studied and applied. However, there are less hydrophilic groups on the surface of carbon-based materials, which make them poor in hydrophilicity [28,33–36].

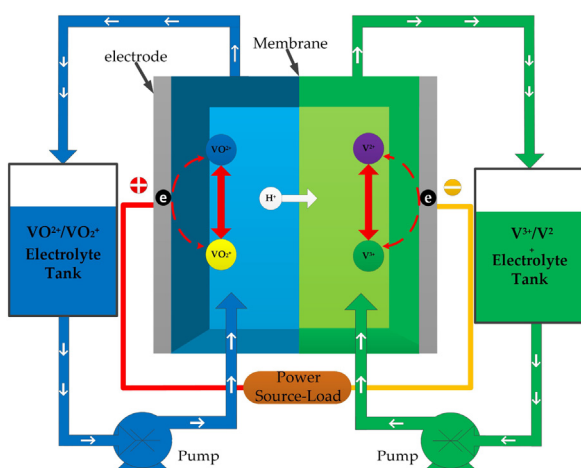


**Fig. 1.** Schematic illustration of the structure of VRFB.

The disadvantage increases the transfer resistance of vanadium ions and decreases working efficiency of VRFB. Therefore, it is very necessary to modify carbon materials before use. Modification of carbon-based materials mainly includes physical and chemical methods, including heat treatment [37], doping treatment [38], acid treatment [39], and introduction of catalysts [40–42]. With further research, modification of carbon-based material by introducing catalyst has gradually become a major research direction. Among them, introduction of metals and metal oxides into electrode surface as catalysts has attracted researchers' attention. In transition metal structure, unpaired *d*-orbital electrons and reactant molecules through electronic contact form various adsorption bonds [43]. These adsorption bonds activate molecules and reduce activation energy of reaction. Due to special band structure of semiconductor material, the reaction products are not easy to be adsorbed on electrode surface, which improves reaction rate on electrode surface [44]. The introduction of metals and metal oxides on surface of electrode material is mainly by chemical methods [45–51]. Metals and metal oxides can be used as catalysts to promote the redox reaction of vanadium ions. Since the metals and metal oxides are loaded, conductivity of carbon-based electrode is effectively improved, and the reaction rate is accelerated [52–54].

Rychcik and Skyllas Kazacos published an article on carbon-polymer composite electrode in 1980s, which began the study of VRFB electrode [55]. Catalyst introduced into electrode surface can provide reaction sites for vanadium ion and promote redox reaction in battery [56–61]. In recent years, there have been a lot of reports about metals and metal oxides modified carbon-based electrode. In this review, we focus on the application of metals and metal oxides modified carbon-based material in VRFB.

## 2. Metal electrocatalysts

### 2.1. Precious metals

Some precious metal catalysts, such as Pt and Ir, are used to modify carbon-based materials and enhance their electrochemical activity [62–65]. Shieh et al. [62] synthesized Pt particles and dispersed them well on multiwalled carbon nanotubes (MWNTs). Fig. 2(a) shows that Pt is evenly distributed on MWNTs and the particle size is small. Pt/MWNT can promote the redox reactions of  $V^{3+}/VO^{2+}$  and  $VO^{2+}/VO_2^+$ . Pt/MWNT improves the coulomb efficiency, energy efficiency of the battery, and reduces overpotential of the reaction (Fig. 2(b)). Pt/C prepared by polyol method has been used as catalyst in fuel battery and other fields [66]. Kwon et al. [63] applied Pt/C catalyst prepared by polyol method to the positive electrode of VRFB to study its catalytic performance. The positively-charged Pt in Pt/C provides active sites for the reaction, which improves efficiency and reduces overpotential and internal resistance. Shieh et al. [64] prepared Pt/C using the immersion reduction method. At the current density of  $10 \text{ mA cm}^{-2}$ , the energy efficiency (EE) of Pt/C (72.3 %) is 20.5 % higher than that of carbon felt (CF). The reaction rate constant of  $VO^{2+}/VO_2^+$  pair on Pt/C is obtained by rotating disk electrode technique. Compared with pristine carbon black, Pt/C has advantages of high reaction rate constant, high reversibility and low overpotential.

Ir is extremely resistant to acids and is the most corrosion resistant metal. Ir is a catalyst with a 5d structure. The research of Wang

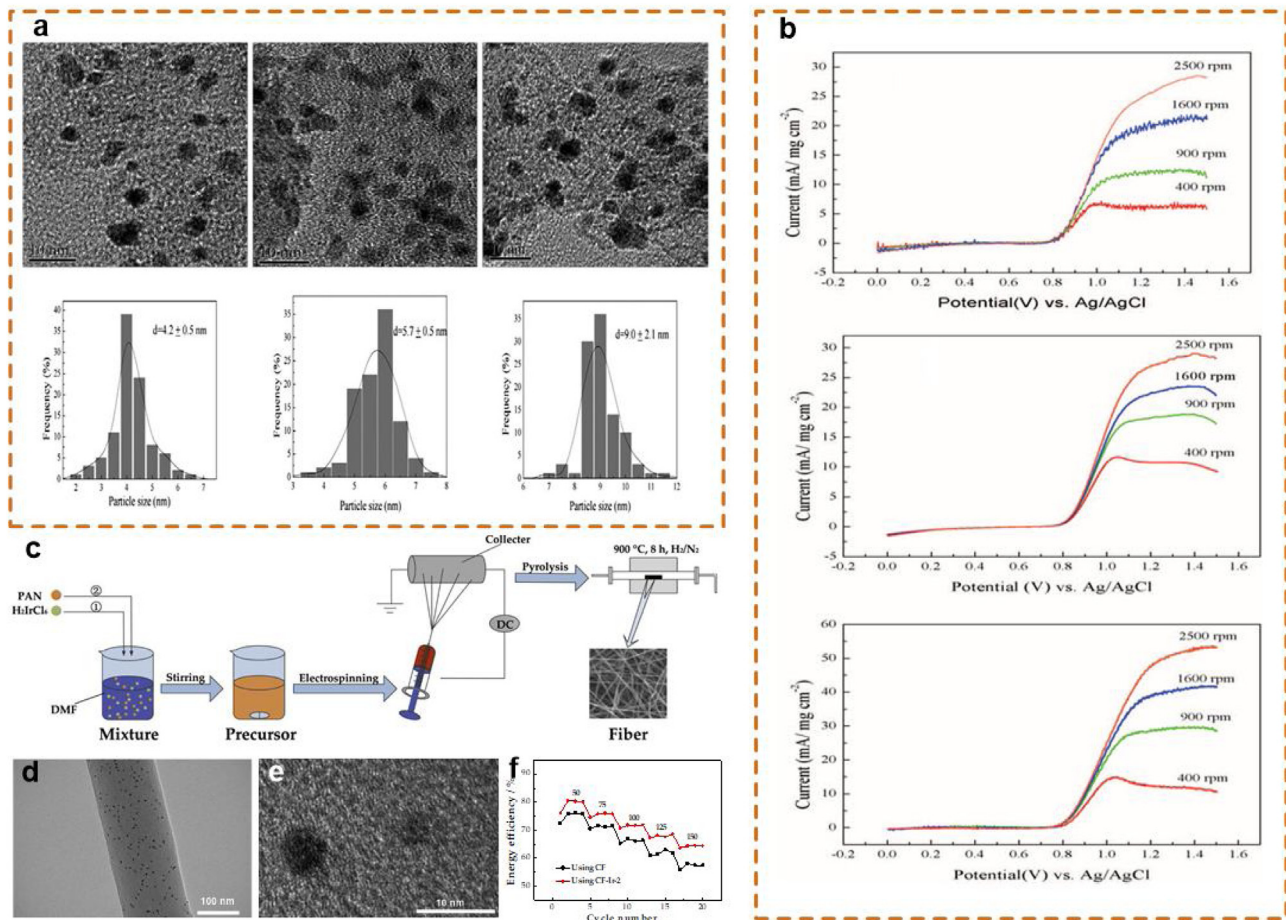


**Fig. 2.** (a) High-resolution transmission electron microscope (TEM) images and particle size histograms, (b) anodic polarization of V(IV) oxidation on different catalysts at different electrode rotating speeds. Reprinted from Ref. [62]. (c) Schematic of the synthesis route for CF-Ir-2, (d) TEM, (e) HR-TEM images of CF-Ir-2, and (f) energy efficiency of the batteries using CF and CF-Ir-2. Reprinted from Ref. [70].

et al. [65] showed that the method of thermal decomposition can change H<sub>2</sub>IrCl<sub>6</sub> into metal Ir and attach it to the surface of CF. After 50 cycles charge-discharge tests, most of Ir remains on the surface of CF, indicating that Ir has good stability in VRFB. Ir-modified CF improves efficiency, and reduces VO<sup>2+</sup>/VO<sub>2</sub><sup>+</sup> reaction overpotential and battery resistance. Ma et al. [67] obtained Ir modified graphene (Ir-G) by synchronous method. Ir has a strong adsorption for oxygen species, which can adsorb VO<sup>2+</sup>/VO<sub>2</sub><sup>+</sup> well [68]. Ir-G has small peak potential difference and low oxidation potential, which improves the electrochemical activity and reversibility of reaction, and improves the energy storage efficiency of the battery [69]. In order to give full play to the catalytic performance of Ir, He et al. [70] used electrospinning technique to embed Ir into carbon fiber (CF-Ir-2) to catalyze the reaction of VO<sup>2+</sup>/VO<sub>2</sub><sup>+</sup>. Fig. 2(c) is a schematic diagram of CF-Ir-2 synthesis route. It can be seen from Fig. 2(d) and (e) that Ir is evenly distributed on CF. The presence of Ir improves EE of the battery. Fig. 2(f) shows that the EE of CF-Ir-2 is 12.2 % higher than that of CF at 150 mA cm<sup>-2</sup>. The discharge capacity of the CF-Ir-2 is 79.5 mA h at the current density of 150 mA cm<sup>-2</sup>. Ir is the most corrosion resistant metal and has good stability in VRFB acid electrolyte [71]. Studies have found that Ir has a significant promotion effect on VO<sup>2+</sup>/VO<sub>2</sub><sup>+</sup> electric pairs, and can be evenly attached to carbon-based materials.

## 2.2. Base metals

Precious metals are expensive and prone to hydrogen evolution reactions, limiting their development. Base metals are inexpensive

and easily available, which have received widespread attention. Some base metals such as Sb, Bi, Cu have been widely used in catalysis [72–76].

Sb is a metal with low cost, corrosion resistance and high catalytic activity. Liu et al. [77] synchronously deposited Sb particles on graphite felt (GF) surface by introducing Sb<sup>3+</sup> into electrolyte. As shown in Fig. 3(a)–(c), the particles continue to accumulate on the GF as the number of cycles increases. Using energy dispersive X-ray spectroscopy (EDX) to analyze particles, as shown in Fig. 3(d), the particles are determined to be Sb. This indicates that the oxidation of Sb is not complete. It can be seen from Fig. 3(e) that accumulated Sb significantly improves the negative performance of VRFB.

Bi has been studied by many researchers for its low toxicity, low cost, good conductivity and stable existence in acid solution. Wang et al. [72] reported that Bi<sup>3+</sup> was reduced to Bi and deposited on GF surface. Bi particles are found at negative electrode after battery operation. It can be found that the electrolyte containing Bi<sup>3+</sup> only catalyzed V<sup>2+</sup>/V<sup>3+</sup> reaction compared with the pristine electrolyte. Blanco et al. [73] proposed a mechanism of the action of Bi particles on VRFB. Thermally treated GF (TTGF) can be considered as a single surface (Fig. 4(a)). Bi-TTGF can be regarded as a system with two different surfaces, which are carbon surface and Bi surface (Fig. 4(a)). Reduction of H<sup>+</sup> on Bi surface will form BiH<sub>3</sub> or BiH<sub>x</sub> compounds (Eq. (3)). BiH<sub>x</sub> does not decompose to form H<sub>2</sub>, but reacts with V<sup>3+</sup> to form V<sup>2+</sup> (Eq. (4)). The total reaction on Bi surface is the reduction of V<sup>3+</sup> to V<sup>2+</sup> (Eq. (5)). Zhang et al. [74] obtained Bi-modified carbon felt by traditional high temperature H<sub>2</sub> reduction method. After heat treatment, the adhesion between

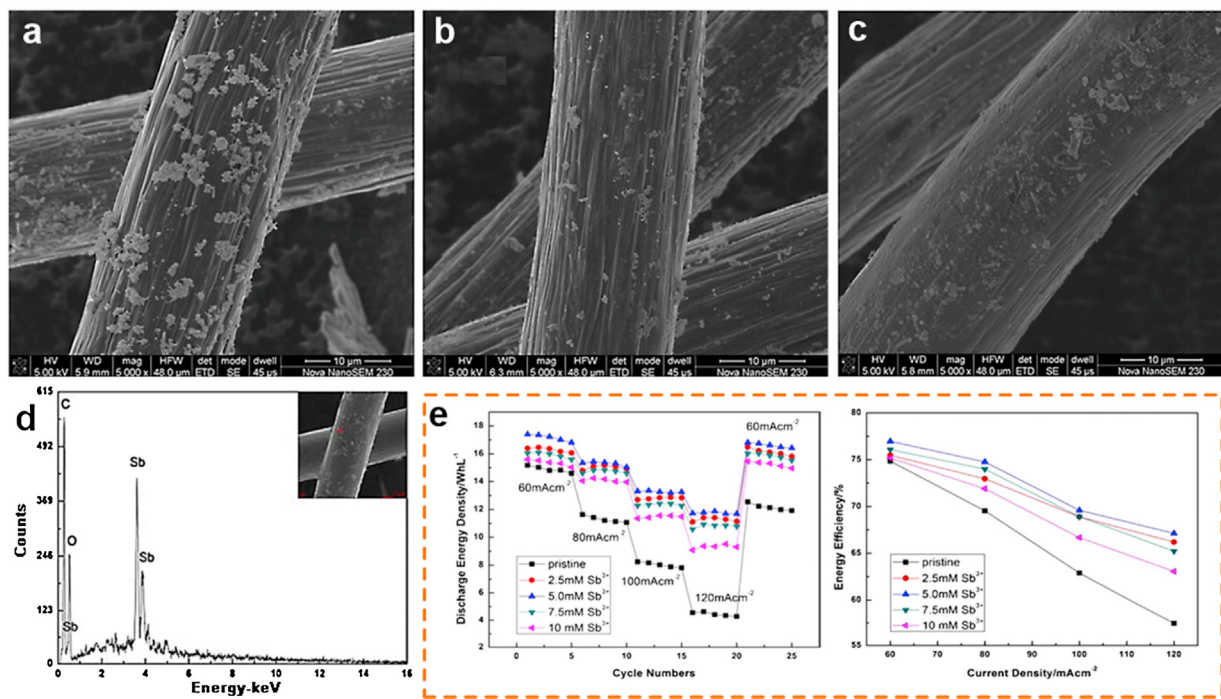


**Fig. 3.** FESEM images of GFs modified with Sb particles at same magnifications after cycling (a) once charge, (b) once charge and discharge and (c) several cycles, (d) EDX spectrogram of particles on the surface of GFs; (e) electrochemical performance of VRFB using electrolyte with different concentrations of Sb<sup>3+</sup> ions. Reprinted from Ref. [77].

CF and Bi is enhanced. In the process of charge-discharge, there is only a small amount of catalyst falling off, which makes the battery keep good stability. Zhao et al. [75] found that oxygen functional groups have an adsorption effect on Bi, which can evenly distribute Bi nanoparticles on the surface of carbon cloth (Fig. 4(c)). As can be seen from Fig. 4(d), the adsorption energy of Bi on the C=O group was 1.32 eV, which is nearly 20 times that of the original carbon cloth (0.07 eV). It can be seen from SEM images (Fig. 4(e)–(h)) that Bi is uniformly attached to the surface of carbon cloth and the particle size is small. Although Bi-modified CF can promote VRFB, the hydrophobicity of CF surface has an adverse effect on distribution and size of Bi [72]. Therefore, Lu et al. [78] pretreated CF with KOH to increase oxygen-containing functional groups and change the surface micropore structure. Bi on the surface of KOH-etched carbon felt is evenly distributed, and the particle size is controlled. CF and GF have different properties. In order to compare their performance, Li et al. [79] introduced Bi to CF and GF surfaces at the same time. They found that CF has a large number of quaternary nitrogen groups and C—OH, which make CF's electrocatalytic activity higher than that of GF.

Bi-modified carbon-based materials are mainly used in VRFB negative electrodes. Santamaria et al. [51] used Bi-modified GF for positive electrode, but the effect is not obvious. This is because the standard redox potential of VO<sup>2+</sup>/VO<sub>2</sub><sup>+</sup> is higher than that of Bi<sup>3+</sup>/Bi. When VO<sup>2+</sup>/VO<sub>2</sub><sup>+</sup> reacts, Bi has been completely oxidized to Bi<sup>3+</sup> and lost its electrochemical activity.

Zhao et al. [76] deposited copper particles on GF surface during charging process by adding a small amount of CuSO<sub>4</sub> to electrolyte. The addition of CuSO<sub>4</sub> only affects negative electrode. This is because the standard potential values of V<sup>3+</sup>/V<sup>2+</sup>, Cu<sup>2+</sup>/Cu, and VO<sup>2+</sup>/VO<sub>2</sub><sup>+</sup> increase in sequence [80]. Before V<sup>3+</sup> is reduced to V<sup>2+</sup>, Cu can be deposited on GF, but not before VO<sup>2+</sup> is oxidized to VO<sub>2</sub><sup>+</sup>. Cu loaded GF improves the performance of battery and the utilization of electrolyte. Sn has good corrosion resistance and can exist stably in acidic solutions. Ha et al. [81] added Sn<sup>2+</sup> into electrolyte and deposited Sn on carbon felt by in-situ electrodeposition. The

deposition of tin has an obvious catalytic effect on the V<sup>3+</sup>/V<sup>2+</sup> reaction. The discharge capacity and energy efficiency of batteries with Sn<sup>2+</sup> added to the electrolyte are improved.

### 3. Metal oxides electrocatalysts

#### 3.1. Transition metal oxides electrocatalysts

##### 3.1.1. IIIB group metal

Lanthanides are widely used as catalyst, where CeO<sub>2</sub> and Nd<sub>2</sub>O<sub>3</sub> are used as catalysts for VRFB. CeO<sub>2</sub> is a semi-open fluorite crystal structure with the advantages of large specific surface area and high defect concentration (such as oxygen vacancies). Qiu et al. [82] prepared modified graphite felts (CeO<sub>2</sub>/GFs) with different CeO<sub>2</sub> contents by precipitation method. It can be seen from Fig. 5(a)–(j) that the addition of CeO<sub>2</sub> improves the roughness of GF surface. The strong interaction between GF and CeO<sub>2</sub> can make CeO<sub>2</sub> disperse uniformly. Fig. 5(k)–(m) shows the introduction of Ce to GF. The introduction of CeO<sub>2</sub> nanoparticles improves hydrophilicity and electrochemical activity of single battery. At the current density of 200 mA cm<sup>-2</sup>, EE of CeO<sub>2</sub>/GF is 64.7 %, which is higher than that of GF (53.9 %). Fan et al. [83] embedded CeO<sub>2</sub> into electrospun carbon nanofibers (ECNFs) through electrospinning technique and high-temperature carbonization. The electrochemical specific surface area of CeO<sub>2</sub>/ECNFs is four times that of ECNFs. From electrochemical test results, CeO<sub>2</sub>/ECNFs can improve electrocatalytic activity for negative reaction of VRFB, but has little effect on positive reaction.

Neodymium has a good combination with oxygen and is an excellent oxygen binder [84]. Fetyan et al. [85] deposited Nd<sub>2</sub>O<sub>3</sub> on CF by precipitation method and proposed the catalytic mechanism of Nd<sub>2</sub>O<sub>3</sub> shown in Fig. 5(n), including the following steps: (a) firstly, due to the strong induction of sulfur and oxygen atoms, Nd<sub>2</sub>O<sub>3</sub> on the surface of CF reacts with SO<sub>4</sub><sup>2-</sup> (electrolyte solution) to form Lewis acid [86]; (b) the formed Lewis acid combines with

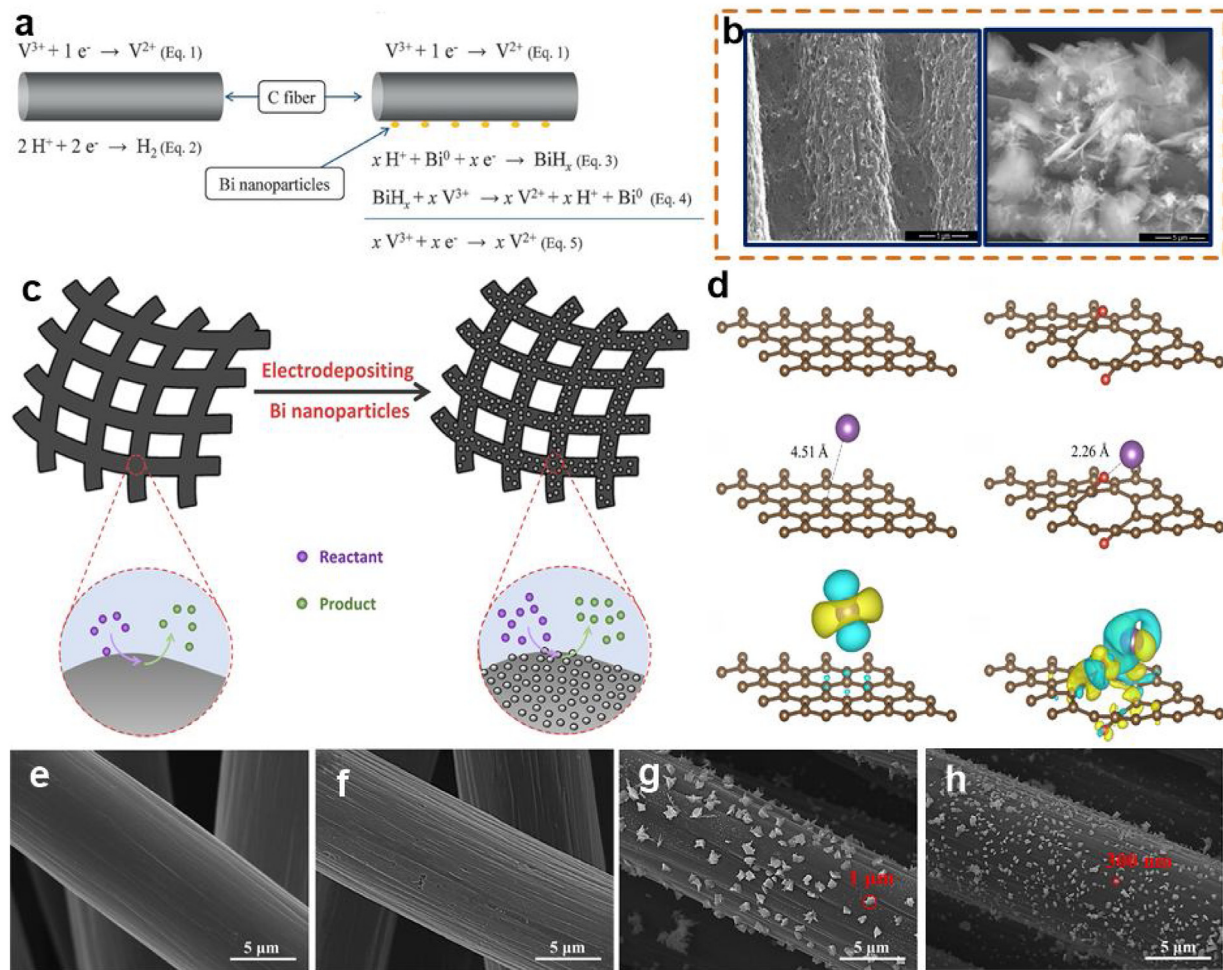


**Fig. 4.** (a) Reaction mechanism of VRFB negative half-cell: on the surface of carbon and bismuth. (b) SEM images of Bi-TTGF and Bi-TTGF after cycling obtained using a secondary electron detector. Reprinted from Ref. [73]. (c) Schematic of the electrode design strategy. (d) different graphite original surface, graphite carbonyl surface schematic diagram and surface adsorption charge difference, SEM images of (e) CC, (f) TCC, (g) BiNP-CC and (h) BiNP-TCC. Reprinted from Ref. [75].

the  $OH^-$  in water to form Bronsted acid center; (c) subsequently, the  $VO_2^{+}$  in reduction process undergoes ion exchange and adsorption reactions with oxygen-containing functional groups on CF to become  $VO_2^{+}$ ; (d) finally, the ions produced by the reaction return to electrolyte. The morphology of  $Nd_2O_3$  is amorphous and distributed on the electrode surface (Fig. 5(o)).  $Nd_2O_3$  has catalytic effect on both positive and negative electrodes.

### 3.1.2. IVB group metal

IVB group metal oxides  $TiO_2$  and  $ZrO_2$  have an important position in the field of catalysis [87–91].  $TiO_2$  is used in photocatalysis [92] and Li-ion batteries [93]. Under acidic conditions,  $TiO_2$  still has good electrochemical characteristics and corrosion resistance. Flox et al. [94] prepared graphite felt-based GF@ $TiO_2$ :H electrode using hydrogenated  $TiO_2$ . Hydrogen treatment forms oxygen vacancies and oxygen functional groups in  $TiO_2$  crystal structure, which improves electrochemical efficiency of  $V^{2+}/V^{3+}$  reaction. Then Flox et al. [95] reported a kind of nitriding  $TiO_2$  carbon felt (CF@ $TiO_2$ ) as negative electrode of VRFB. The synergistic effect of oxygen and nitrogen functionalization on carbon-based surfaces reduces charge transfer resistance. CF@ $TiO_2$ N not only catalyzes  $V^{2+}/V^{3+}$  redox reaction, but also suppresses hydrogen evolution reaction. Wang et al. [96] obtained negative material ( $CNF/TiO_2$ ) which loaded rutile  $TiO_2$  by electrospinning. The synergy between carbon nanofibers (CNF) and rutile  $TiO_2$  makes discharge capacity of

$CNF/TiO_2$  modified battery ( $132.5\text{ mA h}$ ) higher than that of pristine battery ( $84.0\text{ mA h}$ ).  $TiO_2$  has three crystal types: anatase, rutile, and brookite. He et al. [97] studied the effect of anatase  $TiO_2$  ( $\alpha$ - $TiO_2$ ) and rutile  $TiO_2$  ( $\gamma$ - $TiO_2$ ) on negative electrode of VRFB. Compared with  $\gamma$ - $TiO_2$ ,  $\alpha$ - $TiO_2$  lattice has more defects and vacancies, which is conducive to  $V^{2+}/V^{3+}$  reaction. Charge-discharge performance, discharge capacity and energy efficiency of the battery using  $\alpha$ - $TiO_2$  are all improved. Ti and Nb oxides are used as catalysts to promote VRFB, so Wang et al. [98] prepared a catalytic electrical agent using  $TiNb_2O_7$  on reduced graphene oxide ( $TiNb_2O_7$ -rGO). The spatial structure of  $TiNb_2O_7$  is monoclinic. Nb and Ti combine with six oxygen atoms to form an octahedral  $NbO_6$  and  $TiO_6$  with corner and edge sharing, respectively. It can be seen from Fig. 6(a) and (b) that  $TiNb_2O_7$  is fixed uniformly between rGO. Fig. 6(c) shows that the lattice fringe of  $TiNb_2O_7$  is  $0.37\text{ nm}$ , which corresponds to monoclinic  $TiNb_2O_7$ . Fig. 6(d) confirms the existence of  $TiNb_2O_7$ . CV test results (Fig. 6(e)) show that  $TiNb_2O_7$  can promote both positive and negative reactions.

$ZrO_2$  has received considerable attention as a catalyst for various reactions. On the one hand,  $ZrO_2$  has the properties of acidity, alkalinity, oxidability and reducibility. On the other hand,  $ZrO_2$  is also a p-type semiconductor, which is easy to generate oxygen holes [89,99]. Qiu et al. [100] synthesized  $ZrO_2$ -modified GF ( $ZrO_2/GF$ ) by dipping method.  $ZrO_2$  uniformly covers on GF surface, which improves the accessibility of electrolyte and accelerates the reac-

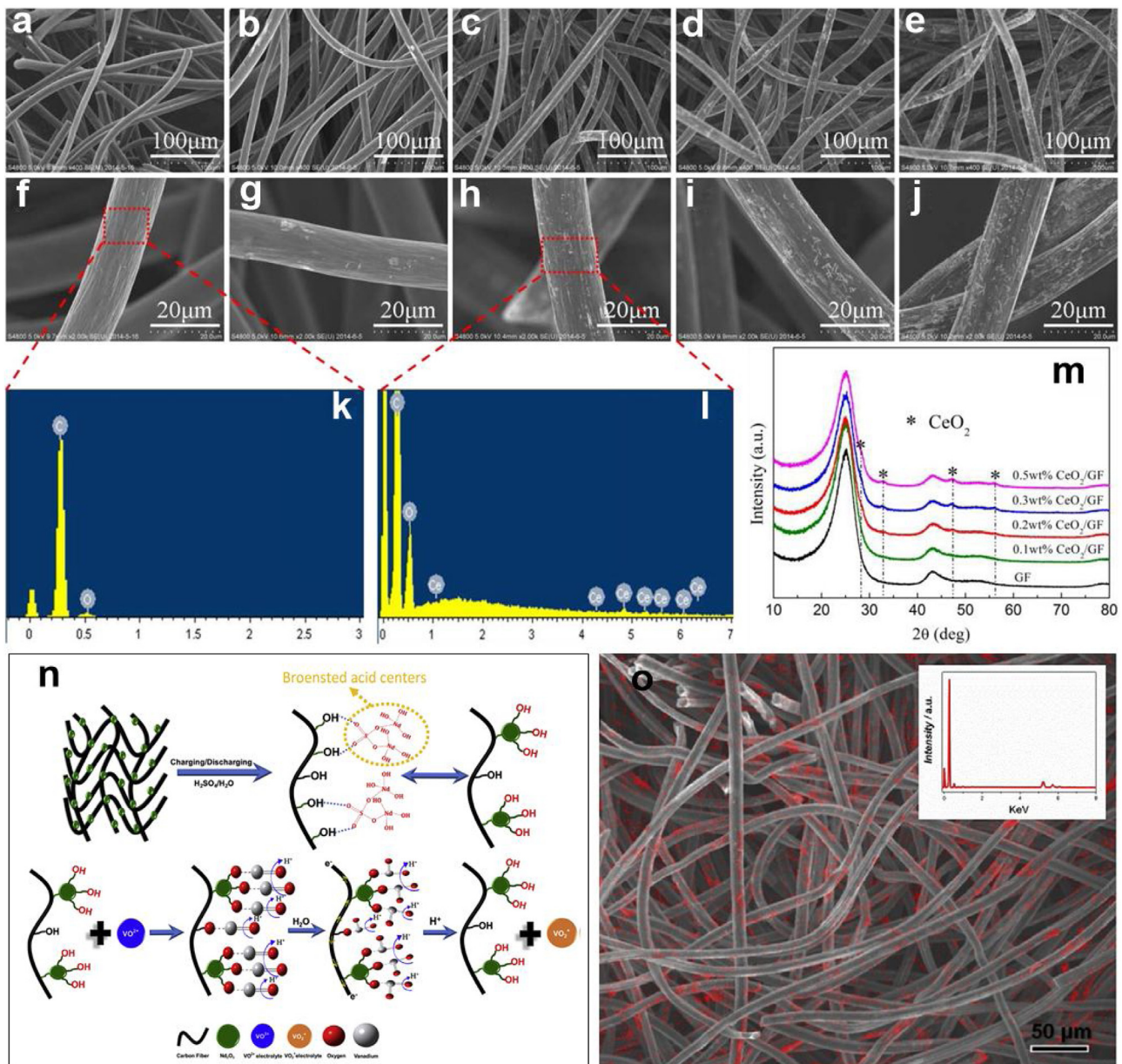


**Fig. 5.** (a–j) SEM images of various electrodes, (k) EDX analysis image of the selective area of GF, (l) EDX analysis image of the selective area of 0.2 wt.% CeO<sub>2</sub>/GF, (m) XRD patterns of the GF and CeO<sub>2</sub>/GF. Reprinted from Ref. [82]. (n) Suggested catalytic mechanism on the Nd<sub>2</sub>O<sub>3</sub>-CF electrodes for VO<sup>2+</sup>/VO<sub>2</sub><sup>+</sup> redox reaction, (o) mapping EDX on selected image of Nd<sub>2</sub>O<sub>3</sub>-CF. Reprinted from Ref. [86].

tion rate. Compared with GF, ZrO<sub>2</sub>/GF has good reversibility for VO<sup>2+</sup>/VO<sub>2</sub><sup>+</sup> and V<sup>2+</sup>/V<sup>3+</sup> redox reactions. Dai et al. [101] uniformly embedded ZrO<sub>2</sub> in carbon nanofibers (CNF), which increases disorder degree of CNF and improves catalytic ability of CNF. After 50 cycles charge-discharge tests at the current density of 80 mA cm<sup>-2</sup>, ZrO<sub>2</sub>/GF modified battery maintains good stability.

IVB group metal oxides TiO<sub>2</sub>, ZrO<sub>2</sub> mainly play a catalytic role in negative electrode of VRFB, but there is little research on the positive electrode. TiO<sub>2</sub> has obvious effect on negative electrode. ZrO<sub>2</sub> has a certain catalytic effect on both positive and negative electrodes. The catalysis of other metal oxides at the same group can be studied.

### 3.1.3. VB group metal

Due to the shrinkage effect of the lanthanide series, Nb and Ta have almost the same atomic size which makes the chemical properties of Nb and Ta very similar. They have good corrosion resistance

and can be stable in the electrolyte. Ta<sub>2</sub>O<sub>5</sub> has a strong adhesion to the electrode surface, and Wang et al. [102] attached Ta<sub>2</sub>O<sub>5</sub> to GF evenly through a one-step hydrothermal method (Fig. 7(a)). When the content of Ta<sub>2</sub>O<sub>5</sub> is 0.75 wt.% (Fig. 7(b) and (c)), Ta<sub>2</sub>O<sub>5</sub> is well dispersed on GF surface. The distance between the lattice fringes is 0.23 nm (Fig. 7(d)), which proves that the particles are Ta<sub>2</sub>O<sub>5</sub>. At the current density of 80 mA cm<sup>-2</sup>, the EE of the battery with 0.75 wt.% Ta<sub>2</sub>O<sub>5</sub>-GF is stable after 100 cycles. The increase of oxygen functional groups on electrode surface can catalyze electrode reaction [59]. Different from other metal oxides, Ta<sub>2</sub>O<sub>5</sub> has four Ta=O and two Ta-O bonds, which may be the reason for its high catalytic activity.

Although Nb has less corrosion resistance than Ta, it is cheaper and more common, so it is often used to replace Ta in some cases. Wang et al. [103] used hydrothermal method to deposit Nb<sub>2</sub>O<sub>5</sub> nanorods on the surface of graphite felt. The results of CV test show that Nb<sub>2</sub>O<sub>5</sub> can catalyze the redox reaction of VO<sup>2+</sup>/VO<sub>2</sub><sup>+</sup> and

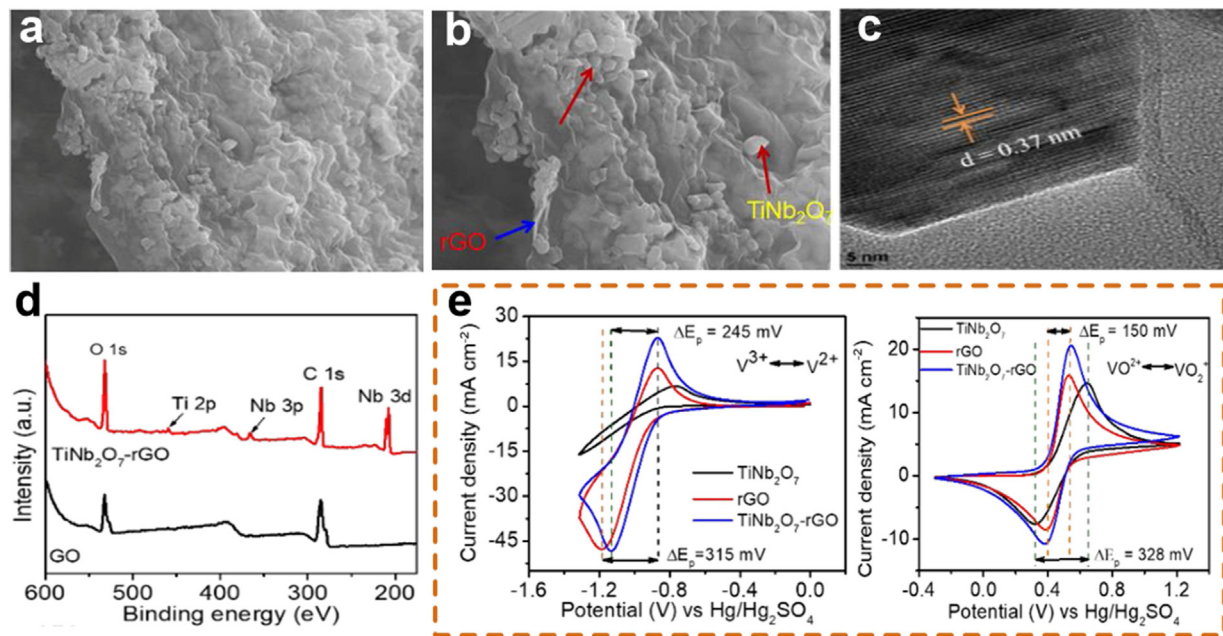


**Fig. 6.** (a, b) FESEM images of  $\text{TiNb}_2\text{O}_7$ -rGO nanocomposites at different magnifications, (c) HRTEM image of  $\text{TiNb}_2\text{O}_7$ -rGO, (d) wide-scan XPS survey, (e) CV curves of the  $\text{TiNb}_2\text{O}_7$ , rGO, and  $\text{TiNb}_2\text{O}_7$ -rGO modified GC electrode. Reprinted from Ref. [98].

$\text{V}^{2+}/\text{V}^{3+}$ .  $\text{Nb}_2\text{O}_5$  has properties of n-type semiconductor, showing poor conductivity. Therefore, W-containing water-soluble compounds were added into the precursor solution to prepare W-doped  $\text{Nb}_2\text{O}_5$  to improve the conductivity. Fig. 7(f) shows that the nanorods are monoclinic. The element composition of nanorods was studied by electron energy loss spectroscopy (EELS). The Nb and W contents are integrated along the green line in Fig. 7(e), and the results are shown in Fig. 7(g). Fig. 7(g) shows that Nb and W are evenly distributed along the axis of the nanorod, which indicates that W is indeed combined with the  $\text{Nb}_2\text{O}_5$  nanorod, rather than simple mixed product of  $\text{WO}_3$  and  $\text{Nb}_2\text{O}_5$ .

### 3.1.4. VIB group metal

In VIB group,  $\text{Cr}_2\text{O}_3$ ,  $\text{MoO}_x$ ,  $\text{WO}_x$  are widely used in VRFB [104–107].  $\text{Cr}_2\text{O}_3$  has advantages of low electromotive force and preventing capacity loss. It is used to improve capacity and stability of battery. Daoud et al. [108] studied a modified method of depositing a thin layer of  $\text{Cr}_2\text{O}_3$  on the surface of GF by immersion combined with ultrasonic. The addition of  $\text{Cr}_2\text{O}_3$  not only inhibits polarization, but also shows good stability in repeated CV test.

Lee et al. [109] used mesoporous carbon foams (MSU-F-C) and  $\text{MoO}_2$  as catalysts ( $\text{MoO}_2/\text{MSU-F-C-2}$ ) to promote  $\text{VO}_2^+/\text{VO}^{2+}$  reaction.  $\text{MoO}_2$  introduces hydrophilic groups on the surface of MSU-F-C to improve hydrophilicity, which accelerates electrolyte diffusion.  $\text{MoO}_2$  is intercalated by metal ions such as  $\text{VO}_2^+/\text{VO}^{2+}$ , which makes the electrode have good conductive effect. Voltage efficiency and energy efficiency of  $\text{MoO}_2/\text{MSU-F-C-2}$  don't decrease with increasing the current density. Even in range of high current density, it has high discharge capacity and small capacity loss. Skyllas-Kazacos et al. [110] assembled  $\text{MoO}_3$  modified CP and electrolyte containing  $\text{MoO}_4^{2-}$  into a battery.  $\text{MoO}_3$  provides the active sites for redox reaction. The addition of  $\text{MoO}_4^{2-}$  also plays a similar role. When current density is  $150 \text{ mA cm}^{-2}$ , power density reaches  $200 \text{ mW cm}^{-2}$ . Whether it is mesoporous carbon foams or carbon paper, compounding with Mo-containing oxide can make VRFB maintain good performance at higher current density.

$\text{WO}_3$  is a kind of n-type semiconductor which can resist light corrosion in aqueous solution. Zhang et al. [104] coated the surface of carbon paper with  $\text{WO}_3/\text{super activated carbon}$  ( $\text{WO}_3/\text{SAC}$ ) by

impregnation method. Compared with pristine carbon paper, the redox reactions of  $\text{VO}_2^+/\text{VO}_2^+$  and  $\text{V}^{2+}/\text{V}^{3+}$  are improved and the transfer resistance is significantly reduced after adding  $\text{WO}_3/\text{SAC}$ . The EE of  $\text{WO}_3/\text{SAC}$  modified battery is  $80.5\%$  at  $50 \text{ mA cm}^{-2}$ , which is higher than that of pristine battery. Nb-doped hexagonal  $\text{WO}_3$  nanowires (Nb-doped h-WO<sub>3</sub> NWs) were synthesized through hydrothermal method by Wang et al. [105]. Nb-doping creates defects in h-WO<sub>3</sub>, forming disordered structures. In the stability test, the battery with Nb-doped h-WO<sub>3</sub> NWs catalyst has almost no attenuation after 30 cycles. Wang et al. [106] also studied that three-dimensionally annealed  $\text{WO}_3$  nanowire/graphene sheet (3D annealed  $\text{WO}_3$  NWs/GS) foam can improve the electrocatalytic activity of positive and negative electrodes of VRFB. This is due to synergistic effect between  $\text{WO}_3$  and GS to form W–O–C bond. At the same time, the annealed  $\text{WO}_3$  NWs/GS foam has three-dimensional porous structure, providing more room for reaction and improving the electrochemical performance. Hosseini et al. [107] reported the promotion effect of N and  $\text{WO}_3$  group-modified carbon-based electrode (HTNW) on VRFB. The electrode preparation method is shown in Fig. 8(a).  $\text{WO}_3$  uniformly covers the electrode surface (Fig. 8(b)). Fig. 8(c) shows that the addition of N has an impact on the chemical environment of the HTNW electrode surface structure. It can be seen from Fig. 8(d) that due to the synergistic effect of N and  $\text{WO}_3$ , charge transfer resistance is reduced from  $76.18 \Omega$  in HT to  $13.00 \Omega$  in HTNW. At high current density of  $200 \text{ mA cm}^{-2}$ , EE of HTNW electrode can reach  $67\%$  (Fig. 8(e)). However, pure  $\text{WO}_3$  has limited active sites, which limits its application in the field of VRFB catalysis [111]. Substoichiometric synthesis forms such as  $\text{W}_{25}\text{O}_{73}$  ( $\text{WO}_{2.92}$ ),  $\text{W}_{5}\text{O}_{14}$  ( $\text{WO}_{2.8}$ ) and  $\text{W}_{18}\text{O}_{49}$  ( $\text{WO}_{2.72}$ ) can be synthesized by etching and generating oxygen vacancies [112]. Among them, the monoclinic phase  $\text{W}_{18}\text{O}_{49}$  is the only known tungsten oxide with the most oxygen defects in the study of nonstoichiometric materials [113]. In view of the performance of  $\text{W}_{18}\text{O}_{49}$ , Wang et al. [114] used it as a catalyst to improve the catalytic performance of GF. At the current density of  $80 \text{ mA cm}^{-2}$ , the EE of modified battery is  $12.5\%$  higher than that of the battery assembled with GF.

In VIB group, there are many studies on  $\text{WO}_3$  as a VRFB electrode catalyst, and  $\text{WO}_3$  has a positive effect on electrode reaction. The

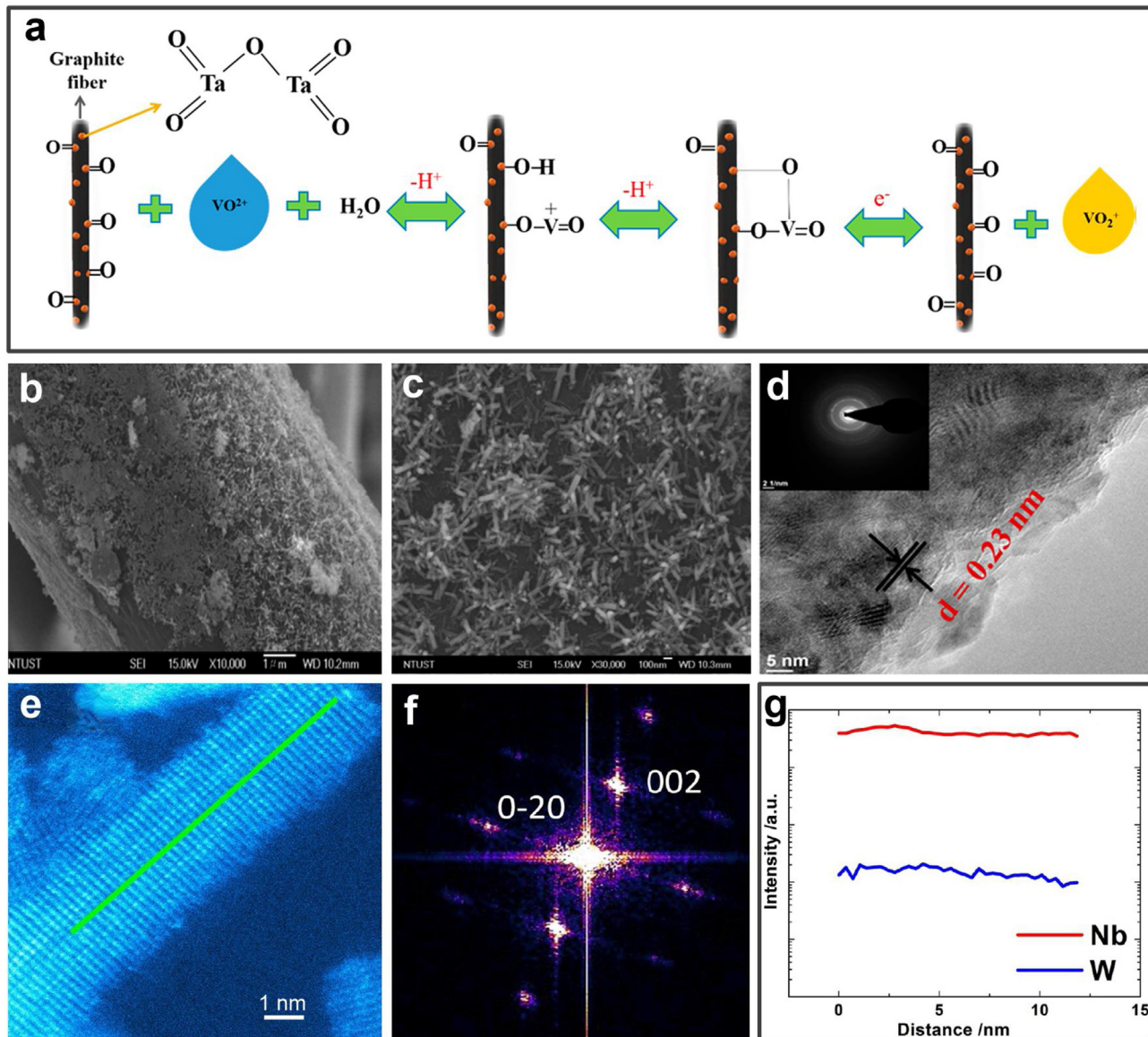


**Fig. 7.** (a) Schematic diagram of redox mechanism of  $\text{VO}^{2+}/\text{VO}_2^+$  with  $\text{Ta}_2\text{O}_5$  on GF electrode surface. (b, c) SEM images of 0.75 wt.%  $\text{Ta}_2\text{O}_5$ -GF. (d) high-resolution TEM image and the corresponding selected area electron diffraction (SAED) pattern (the inset). Reprinted from Ref. [102]. (e) STEM image of W-doped  $\text{Nb}_2\text{O}_5$  nanorods, (f) corresponding FFT of one atomic resolution image (panel e), (g) distributions of Nb and W elements in one EELS line scan (the line is shown in panel e). Reprinted from Ref. [103].

oxides of Cr and Mo are mainly used in positive electrode. The same group of elements has similar properties. We can try to apply them to negative electrode.

### 3.1.5. VIIB group metal

Manganese oxide has excellent cation exchange capacity and characteristics in electrochemical and magnetic properties. These characteristics make it widely used in redox catalysis, molecular sieves, positive materials of lithium batteries and magnetic materials [115,116]. Kim et al. [117] prepared  $\text{Mn}_3\text{O}_4$  modified GF electrode by hydrothermal method and applied it to VRFB for the first time. The test results confirm that  $\text{Mn}_3\text{O}_4$  modified GFs as positive and negative electrodes of the battery reduce overpotential of reaction and improve voltage, coulomb and energy efficiency of battery. Compared with hydrothermal method, electrodeposition is an efficient and simple method. Zhao et al. [118] obtained  $\text{Mn}_3\text{O}_4$  modified carbon cloth ( $\text{Mn}_3\text{O}_4/\text{CCs}$ ) by electrodeposition and heat treatment.  $\text{Mn}_3\text{O}_4/\text{CCs}$  has obvious catalytic effect on  $\text{V}^{2+}/\text{V}^{3+}$  reaction. At the current density of  $100 \text{ mA cm}^{-2}$ , the EE of  $\text{Mn}_3\text{O}_4/\text{CCs}$

modified battery reached 88 %, which is 17 % higher than that of pristine battery. Blasi et al. [119] used electrospinning technique to prepare  $\text{Mn}_3\text{O}_4$  modified CNF ( $\text{Mn}_3\text{O}_4/\text{CNF}$ ). The results show that  $\text{Mn}_3\text{O}_4/\text{CNF}$  has good catalytic effect on  $\text{VO}^{2+}/\text{VO}_2^+$  and  $\text{V}^{2+}/\text{V}^{3+}$  electric pairs. Because of its low conductivity and weak adhesion,  $\text{Mn}_3\text{O}_4$  needs to work with high conductivity carrier. Multi-walled carbon nanotubes (MWCNTS) have excellent electrical conductivity. Liu et al. [120] introduced  $\text{Mn}_3\text{O}_4$  to the surface of MWCNTS as positive electrode catalyst by hydrothermal method. After 50 cycles, energy efficiency of  $\text{Mn}_3\text{O}_4/\text{MWCNTs}$  modified battery (84.65 %) is 3.73 % higher than that of pristine battery. Liu et al. [121] fixed  $\text{Mn}_3\text{O}_4$  with bifunctional polydopamine (PDA). Bifunctional polydopamine can not only fix  $\text{Mn}_3\text{O}_4$  nanoparticles on GF, but also increase the  $\text{VO}^{2+}/\text{VO}_2^+$  redox reaction rate. Compared with pure PDA and pure  $\text{Mn}_3\text{O}_4$ , PDA- $\text{Mn}_3\text{O}_4$  has the highest electrocatalytic performance due to its synergistic effect. It is a new trend to develop the synergy between electrocatalyst and support. Walsh et al. [122] synthesized a synergistic nitrogen-doped reduced graphene oxide/ $\text{Mn}_3\text{O}_4$  ( $\text{N}-\text{rGO}-\text{Mn}_3\text{O}_4$ ) catalyst. CV tests

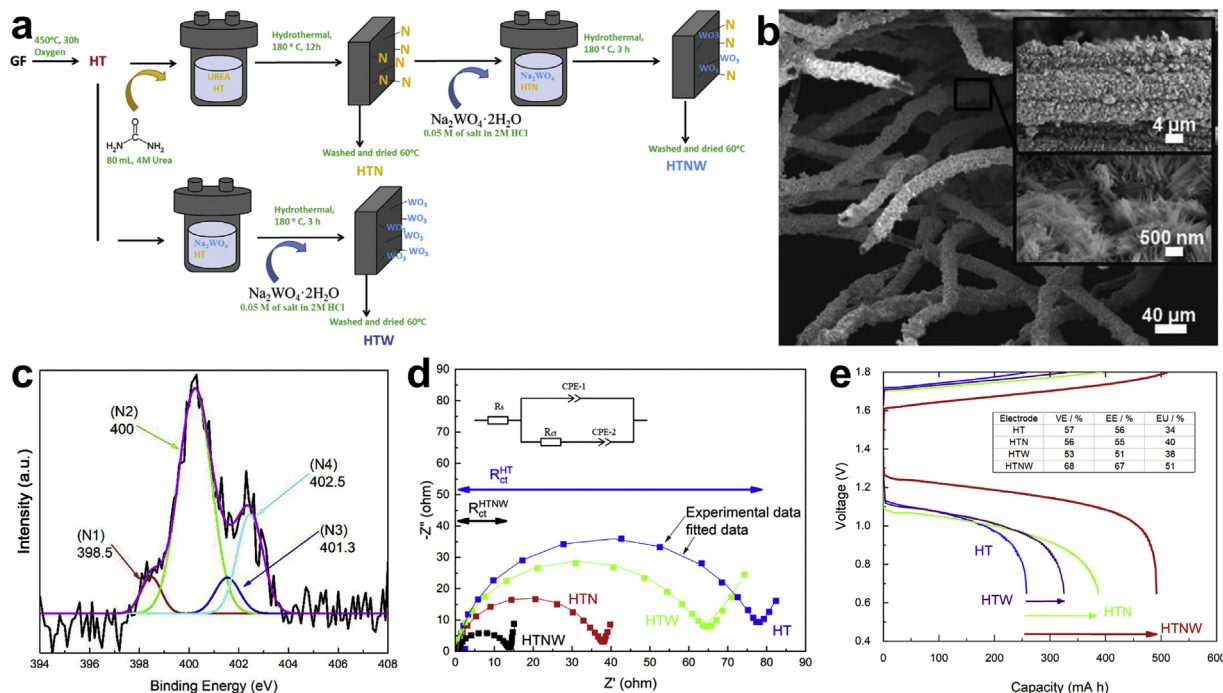


**Fig. 8.** (a) Illustration of the electrode preparation, (b) morphologies of HTNW electrodes, (c) XPS for N 1s spectra for HTNW electrodes, (d) Nyquist impedance plots of different carbon felt electrodes, (e) comparison of the electrochemical performance for all as-prepared electrodes, showing the voltage profiles for charge and discharge process at 200 mA cm<sup>-2</sup>. Reprinted from Ref. [107].

find that the catalytic performance of N-rGO-Mn<sub>3</sub>O<sub>4</sub> is higher than that of N-rGO or Mn<sub>3</sub>O<sub>4</sub> alone.

As another manganese oxide, MnO<sub>2</sub> is also used in the field of VRFB. Wu et al. [123] prepared graphite felt/MnO<sub>2</sub> (GF-MNO) composite electrode by one-step hydrothermal method under acidic condition to catalyze the redox reaction of VO<sup>2+</sup>/VO<sub>2</sub><sup>+</sup>. Compared with GF, the energy efficiency and discharge capacity of GF-MNO at 150 mA cm<sup>-2</sup> are increased by 12.5 % and 40 %, respectively. He et al. [124] used in-situ deposition method to obtain MnO<sub>2</sub> modified carbon paper for VRFB negative electrode. In Fig. 9(a) and (d), the nanosheets are completely coated on CP. From the lattice fringes in different directions in Fig. 9(b) and (e), it is found that the nanoflakes are MnO<sub>2</sub>. It can be clearly seen from Fig. 9(c) and (f) that water droplets show hydrophobic on CP surface, while rapidly spread on MnO<sub>2</sub> modified CP surface. MnO<sub>2</sub> nanosheets provide many active sites for V<sup>2+</sup>/V<sup>3+</sup> redox reaction, improve hydrophilicity of carbon paper, and promote the progress of reaction (Fig. 9(g)-(i)).

Manganese oxide is a kind of material with low cost, high catalytic efficiency, no pollution and easy to get, which has been widely studied. Manganese oxide can exist stably under acidic conditions and has good catalytic properties, which has broad prospects in the field of VRFB.

### 3.1.6. VIII group metal

Although Pt, Ir and other metals can improve performance of VRFB, their high cost and poor mechanical stability limit their industrial development. Researchers turned their attention to other metals in the same group. It is found that the oxides of Co, Ni and Ru have better electrochemical performance, which are expected to replace precious metals gradually.

Daoud et al. [125] loaded a thin layer of CoO on the surface of GF (CoTGF) to catalyze the redox reaction of VO<sup>2+</sup>/VO<sub>2</sub><sup>+</sup>. After 50 cycles of CV test, the peak shift of CoTGF electrode did not change significantly, indicating that CoO can stably exist on graphite felt surface.

The discharge capacity of VRFB increased from initial 185.4–373.9 mA h after modification, which improved the battery efficiency.

Yang et al. [126] uniformly prepared high performance NiO catalyst on GF and confirmed its positive and negative effects on VRFB. NiO improves hydrophilicity of GF, reduces reaction resistance and further improves electrochemical activity of the reaction. Under different current densities, the performance of NiO/GF modified battery has been improved in all aspects. Especially under high current density of 125 mA cm<sup>-2</sup>, the EE value of NiO/GF is 74.5 %, which is 19.1 % higher than that of pristine battery. In addition, NiO/GF has good corrosion resistance and stability in acid solution. Parka et al. [127] used NiO/Ni redox to prepare high pore GF electrodes to promote the redox reaction of V<sup>2+</sup>/V<sup>3+</sup> and VO<sup>2+</sup>/VO<sub>2</sub><sup>+</sup>. Etched graphite felt (EGF) has a high specific surface area and stepped edges, which provides a place for incorporating oxygen defects. Fig. 10(a)–(c) shows the process and formation mechanism of EGF. The structure of EGF<sub>3</sub> is shown in Fig. 10(d). The oxygen defects of EGF can improve wettability of electrode to electrolyte and reduce over potential of reaction. Discharge capacity and EE of EGF<sub>3</sub> battery are higher than that of other two batteries, and there is no significant attenuation within 50 cycles. In addition, the surface morphology of EGF<sub>3</sub> did not change after reaction, leaving original porous structure and defects. This shows that EGF<sub>3</sub> has good stability in acid environment.

The conductivity of a single metal oxide is low. As a composite metal oxide with a reverse spinel structure, NiCoO<sub>2</sub> has much higher electrochemical catalytic performance than single NiO or CoO. Daoud et al. [58] used NiCoO<sub>2</sub> as the positive catalyst of VRFB to study its performance. At the current density of 150 mA cm<sup>-2</sup>, the EE of batteries modified by NiCoO<sub>2</sub>, CoO and pristine GF is 72.5 %, 69.2 % and 57 %, respectively. Binary metal oxide NiCoO<sub>2</sub> has higher electrocatalytic activity and conductivity.

RuO<sub>2</sub> has high electrocatalytic performance and good stability in acid environment. The nature of RuO<sub>2</sub> is related to its morphology (oxidation and hydration). Therefore, Faraji et al. [128] combined RuO<sub>2</sub> with MWCNT supported by Stainless Steel Mesh (SSM) to

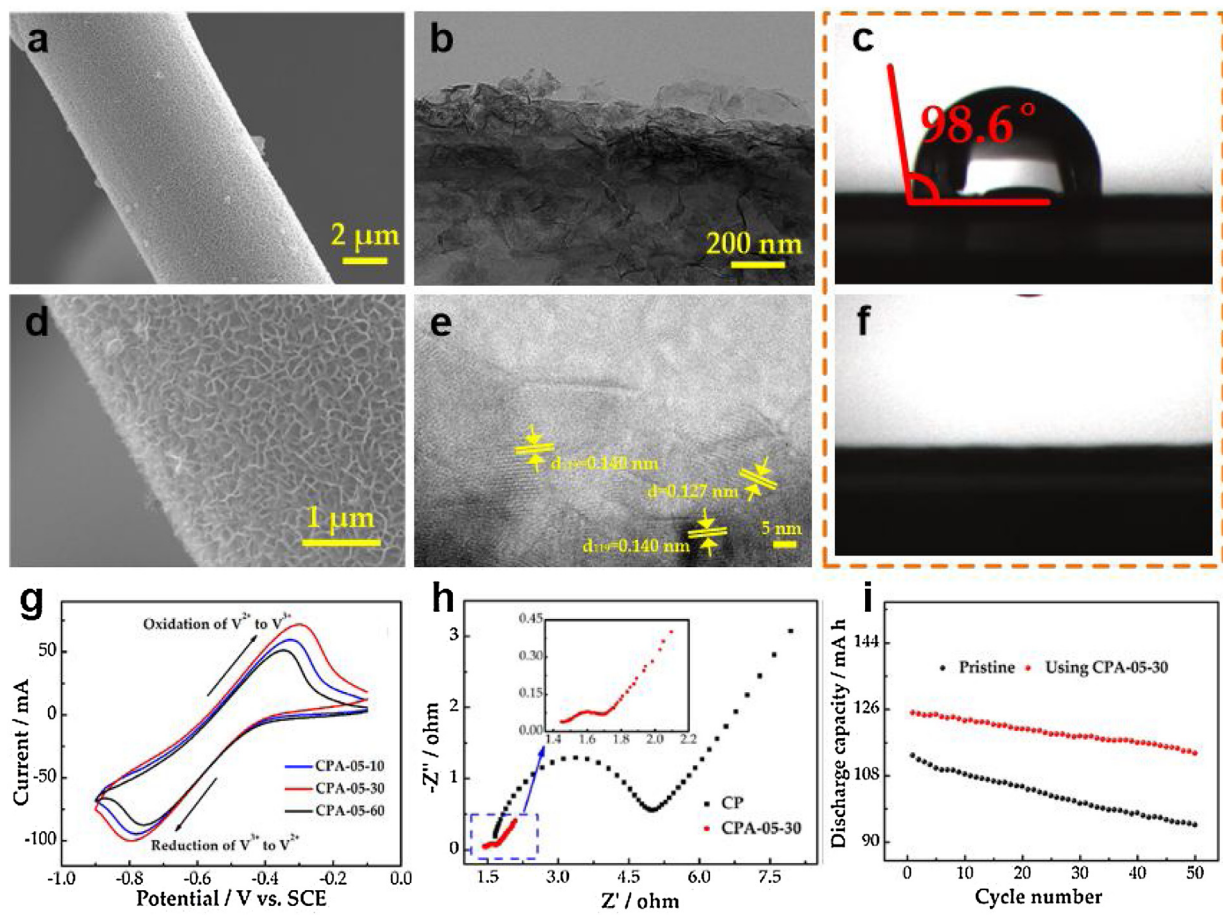


**Fig. 9.** (a, d) SEM images of CPA-05-30, (b) TEM and (e) high-resolution TEM images of CPA-05-30, cross-sectional view of the water droplet on (c) CP and (f) CPA-05-30, (g, h, i) electrochemical performance of VRFB. Reprinted from Ref. [124].

prepare RuO<sub>2</sub>/MWCNT/SSM catalyst for positive electrode. In CV test, RuO<sub>2</sub>/MWCNT/SSM electrode has higher peak current, faster electron transfer rate, and smaller peak potential difference. At the current density of 500 mA g<sup>-1</sup>, the electrode maintains 91 % specific discharge capacity after 10 days of use. Because the cost of RuO<sub>2</sub> is higher than that of other oxide catalysts, if RuO<sub>2</sub> is to be industrialized, it must have higher catalytic performance.

### 3.2. Main group metal oxides: IVA group metal

The main group metal oxides catalysts are acid-base catalysts, which are rarely studied in the field of VRFB catalysis. PbO<sub>2</sub> has two crystal forms:  $\alpha$ -PbO<sub>2</sub> and  $\beta$ -PbO<sub>2</sub>.  $\beta$ -PbO<sub>2</sub> has good corrosion resistance and electrical conductivity, which is often used as surface active layer of electrodes.  $\alpha$ -PbO<sub>2</sub> has strong binding force, which can make PbO<sub>2</sub> and GF have good contact. Xu et al. [129] prepared  $\alpha$ -PbO<sub>2</sub> and  $\beta$ -PbO<sub>2</sub> composite PbO<sub>2</sub> modified graphite felt electrode. Compared with pristine battery, the VE and EE of PbO<sub>2</sub> modified battery have been greatly improved.

SnO<sub>2</sub> is a kind of n-type semiconductor, which has the properties of amphoteric oxide, good hydrophilicity and electrochemical stability. It has a wide range of applications in battery electrodes, optics and other fields [130–132]. Ha et al. [133] made an evaluation on carbon felt electrode which was decorated with SnO<sub>2</sub> nanoparticles. The preparation diagram is shown in Fig. 11(a). It can be seen from Fig. 11(b)–(e) that SnO<sub>2</sub> is distributed on the surface of carbon fiber. The presence of SnO<sub>2</sub> nanoparticles reduces reaction potential and charge transfer resistance, and has a significant

effect on VO<sup>2+</sup>/VO<sub>2</sub><sup>+</sup>. At the current density of 150 mA cm<sup>-2</sup>, the EE of SnO<sub>2</sub> modified battery is 77.3 %, which is 23.7 % higher than that of pristine battery. Compared with pristine electrode, cycling stability of the system is improved by approximately 2.7 times at the current density of 50 mA cm<sup>-2</sup>. A simultaneous nano etching and SnO<sub>2</sub> loading on the surface of carbon fiber (SnPc) to enhance redox reaction of vanadium ion was prepared by Jun et al. [134]. CV test results show that SnPc can improve positive and negative electrode responses of VRFB. He et al. [135] prepared SnO<sub>2</sub> modified carbon paper as VRFB dual function electrode by two-step method. The battery with CP/SnO<sub>2</sub> as electrode was charged and discharged for 50 times, and the stability and capacity retention rate remained well. The discharge capacity for CP/SnO<sub>2</sub> can reach 86.8 mA h at the current density of 150 mA cm<sup>-2</sup>. The battery using CP/SnO<sub>2</sub> shows high energy and voltage efficiency. In order to further improve the catalytic performance of SnO<sub>2</sub>, He et al. [136] prepared Sb doped SnO<sub>2</sub> on carbon paper (CP-SnO<sub>2</sub>/Sb) by electrodeposition (Fig. 11(f)). It can be seen from Fig. 11(g)–(i) that the addition of Sb makes the particle distribution on the surface of carbon fiber more uniform and the particle size smaller, which provide more active sites for the reaction.

PbO<sub>2</sub> and SnO<sub>2</sub> are both n-type semiconductors, and electrons are easily excited into the conduction band to generate free electron conduction. The generation of free electrons enhances the conductivity of electrode materials and improves the performance of VRFB. SnO<sub>2</sub> can promote the positive and negative reactions of VRFB, but there is little research on the application of PbO<sub>2</sub> in positive electrode.

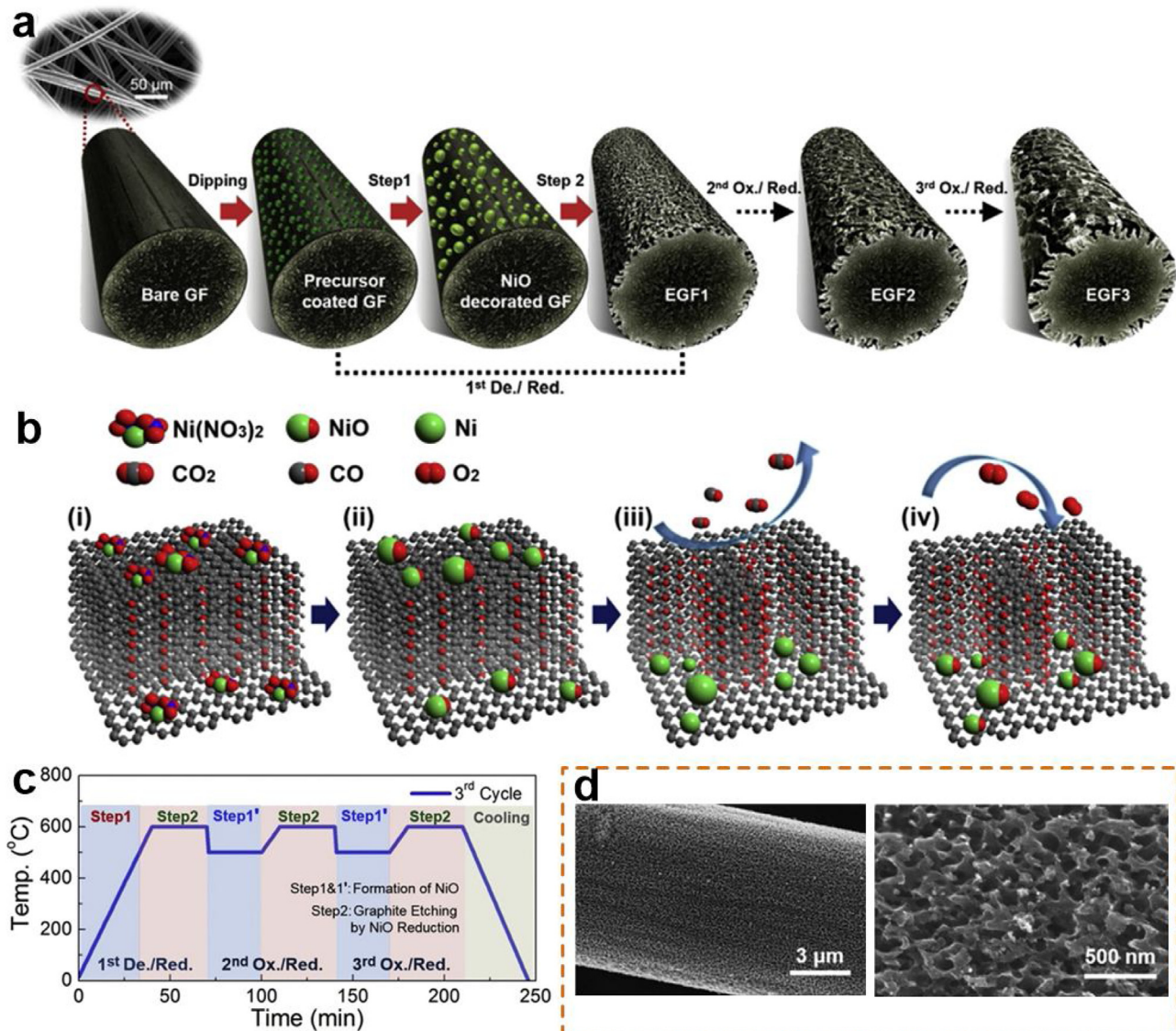


**Fig. 10.** (a) Preparation steps of etched graphite (EGF) from bare graphite felt (BF) by the redox reaction of NiO/Ni, (b) etching mechanism of graphitic surface by the redox reaction of NiO/Ni, (c) operating-temperature profiles for three cycles of the NiO/Ni redox reaction, (d) SEM images of EGF<sub>3</sub>. Reprinted from Ref. [127].

#### 4. Conclusion and perspectives

There are many unstable factors in some commonly used renewable energies, which are difficult to be directly applied. As a new type of large-scale energy storage device, VRFB has the function of storing unstable electric energy. Electrode material is one of the key components that affects and restricts the performance of VRFB. By modifying metals and metal oxides on the surface of carbon-based materials, the electrochemical properties of electrode materials, such as reaction kinetics, voltage efficiency and energy efficiency, can be effectively improved. But their catalytic activity and cycle stability still need to be further improved. It is a research hotspot to restrain the side reactions of hydrogen evolution and oxygen evolution by attaching metals and metal oxides on the surface of carbon-based material. In order to improve the performance of the battery and develop the potential of electrode application, the following prospects are proposed:

(1) In the environment of strong acid and strong oxidation, the dissolution and shedding of metals and metal oxides will

lead to the degradation of catalytic performance. Low-cost, high-conductivity, high catalytic activity and stable integrated electrode is the future development trend. By means of hot pressing and bonding, the modified graphite felt electrode and collector are bonded together, which reduces the contact resistance between the electrode and collector, simplifies the assembly of the battery and improves the voltage efficiency of VRFB.

(2) In addition to the commonly used hydrothermal, acid treatment and other electrode modification methods, there are some methods that can have a great effect on electrode optimization. For example, microwave treatment is the most efficient and environmentally friendly method for improving the electrochemical activity of GF. By microwave treatment, GF has more hydrophilic groups on its defects, and excellent properties. Metal organic framework material (MOFs) is a kind of coordination polymer with three-dimensional pore structure. Generally, metal ions are used as the connection points, and the organic coordination body supports the 3D extension of space. MOFs is an important new type of porous material, which is

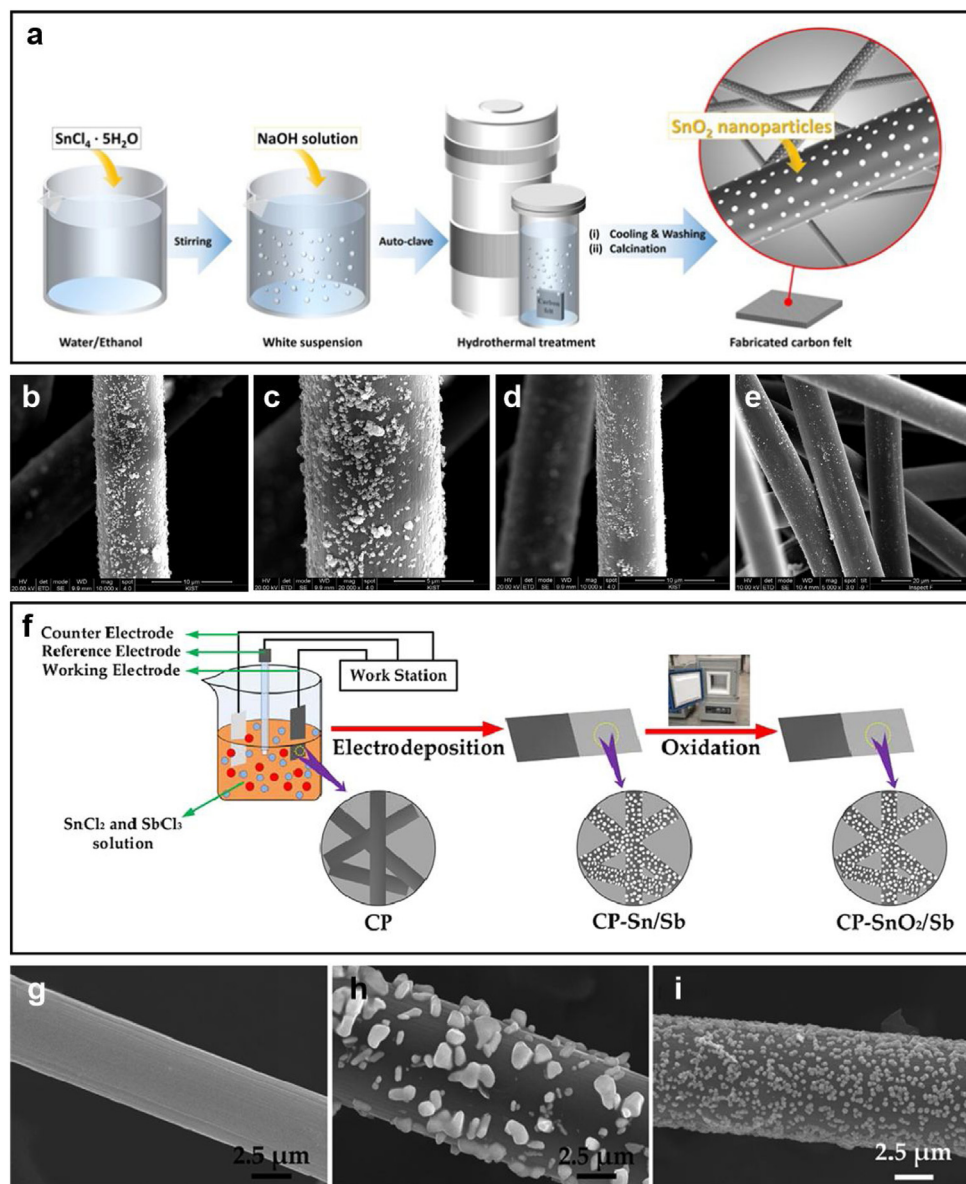


**Fig. 11.** (a) Schematic of the synthesis of SnO<sub>2</sub> nanoparticle-deposited CF, (b–e) various magnifications of the SnO<sub>2</sub> deposited onto the CF. Reprinted from Ref. [133]. (f) Process diagram of SnO<sub>2</sub>/Sb modified carbon paper, SEM images of (g) CP, (h) CP-SnO<sub>2</sub>, and (i) CP-SnO<sub>2</sub>/Sb. Reprinted from Ref. [136].

widely used in catalysis, energy storage and separation. MOFs has good catalytic performance and can be used in VRFB in the future.

(3) The oxygen-containing functional group can be added at the same time as the introduction of the metal catalyst. Oxygen-containing functional groups can improve the stability of metals and have a synergistic effect with metals. But some precious metals are expensive and prone to hydrogen evolution. Therefore, we need to explore other low-cost and high-performance metal-based catalysts. Metal oxide has better catalytic performance, but poor conductivity. Combining metal oxides with highly conductive carbon nanotubes or graphene, they can play a synergistic effect to improve the catalytic activity of the material. Develop some binary metal oxides, such as TiNb<sub>2</sub>O<sub>5</sub>, ZrCeO<sub>2</sub> and NiCoO<sub>2</sub>. The properties of binary metal oxides are higher than that of single metal oxides. Some metal compounds such as metal phosphides, metal nitrides and metal carbides are also used in VRFB. These metal compounds have significantly improved conductivity compared to metal oxides.

(4) Although a lot of researches have been devoted to the modification of electrode, such work has increased the production steps and costs of electrode invisibly. Therefore, it is necessary to actively explore simple electrode optimization methods and strengthen the research of electrode body performance, which not only provides the basis for the selection of electrode materials, but also is one of the development directions of electrode materials.

#### Declaration of Competing Interest

The authors declare that they have no known competing financial interests or personal relationships that could have appeared to influence the work reported in this paper.

#### Acknowledgements

This work was financially supported by the National Natural Science Foundation of China (Nos. 51872090 and 51772097) and the

Hebei Natural Science Fund for Distinguished Young Scholar (Nos. E2019209433 and E2017209079).

## Appendix A. Supplementary data

Supplementary material related to this article can be found, in the online version, at doi:<https://doi.org/10.1016/j.jmst.2020.09.042>.

## References

- [1] K.L. Huang, X.G. Li, S.Q. Liu, N. Tan, L.Q. Chen, Renew. Energy 33 (2008) 186–192.
- [2] L. Wang, X. Xie, K.N. Dinh, Q.Y. Yan, J.M. Ma, Coord. Chem. Rev. 397 (2019) 138–167.
- [3] Y. Shao, X. Wang, M. Engelhard, C. Wang, S. Dai, J. Liu, Z. Yang, Y. Lin, J. Power Sources 195 (2016) 4375–4379.
- [4] J. Huang, J. Shen, S. Li, J. Cai, S. Wang, Y. Lu, J. He, C.J. Carmalt, I.P. Parkin, Y. Lai, J. Mater. Sci. Technol. 39 (2020) 28–38.
- [5] J. Zhang, X. Yao, R.K. Misra, Q. Cai, Y. Zhao, J. Mater. Sci. Technol. 44 (2020) 237–257.
- [6] Y. Li, Y. Feng, X. Sun, Y. He, Angew. Chem. 56 (2017) 5734–5737.
- [7] M. Haider, C. Zhen, T. Wu, G. Liu, H.M. Cheng, J. Mater. Sci. Technol. 34 (2018) 1474–1480.
- [8] M. Li, N. Yuan, Y. Tang, L. Pei, Y. Zhu, J. Liu, L. Bai, M. Li, J. Mater. Sci. Technol. 35 (2019) 604–609.
- [9] C.C. Li, B. Zhang, Q.X. Liu, J. Energy Storage 29 (2020), 101339.
- [10] L.A.W. Ellingsen, C.R. Hung, A.H. Stromman, Transp. Res. 55 (2017) 82–90.
- [11] Y. Zhao, Y. Ding, Y. Li, L. Peng, H.R. Byon, J.B. Goodenough, G. Yu, Chem. Soc. Rev. 44 (2015) 7968–7996.
- [12] P. Leung, X. Li, C.P. de Leon, B. Berlouis, C.T.J. Low, F.C. Walsh, RSC Adv. 2 (2012) 10125–10156.
- [13] W. Weng, L. Tang, W. Xiao, J. Energy Chem. 28 (2019) 128–143.
- [14] J. Ma, S. Shi, X. Jia, F. Xia, H. Ma, J. Gao, J. Xu, J. Energy Chem. 36 (2019) 74–86.
- [15] E.X. Han, Y.Y. Li, Q.H. Wang, W.Q. Huang, L. Luo, W. Hu, G.F. Huang, J. Mater. Sci. Technol. 35 (2019) 2288–2296.
- [16] E. Lantos, L. Merai, A. Deak, J. Gomez-Perez, D. Sebok, I. Dekany, Z. Konya, L. Janovak, J. Mater. Sci. Technol. 41 (2020) 159–167.
- [17] C. Yan, J. Huang, C. Wu, Y. Li, Y. Tan, L. Zhang, Y. Sun, X. Huang, J. Xiong, J. Mater. Sci. Technol. 42 (2020) 10–16.
- [18] Z. Yang, J. Zhang, M.C.W. Kintner-Meyer, X. Lu, D. Choi, J.P. Lemmon, J. Liu, Chem. Rev. 111 (2011) 3577–3613.
- [19] J. Liu, J.G. Zhang, Z. Yang, J.P. Lemmon, C. Imhoff, G.L. Graff, L. Li, J. Hu, C. Wang, J. Xiao, G. Xia, V.V. Viswanathan, S. Baskaran, V. Sprenkle, X. Li, Y. Shao, B. Schwenger, Adv. Funct. Mater. 23 (2013) 929–946.
- [20] S. Chu, A. Majumdar, Nature 488 (2012) 294–303.
- [21] X. Xu, H. Tan, K. Xi, S. Ding, D. Yu, S. Cheng, G. Yang, X. Peng, A. Fakih, R.V. Kumar, Carbon 84 (2015) 491–499.
- [22] W. Ai, Z. Luo, J. Jiang, J. Zhu, Z. Du, Z. Fan, L. Xie, H. Zhang, W. Huang, T. Yu, Adv. Mater. 26 (2014) 6186–6192.
- [23] B. Dunn, H. Kamath, J.M. Tarascon, Science 334 (2011) 928–935.
- [24] C.C. Li, B. Zhang, B.S. Xie, X.B. Zhao, J. Chen, Energy Convers. Manage. 208 (2020) 112586–112595.
- [25] W. Wang, Q. Luo, B. Li, X. Wei, L. Li, Z. Yang, Adv. Funct. Mater. 23 (2013) 970–986.
- [26] Z. Wei, A. Bhattacharai, C. Zou, S. Meng, M. Skyllas-Kazacos, J. Power Sources 390 (2018) 261–269.
- [27] A. Fetyan, G.A. El-Nagar, I. Lauermann, M. Schnucklaje, J. Schneider, C. Roth, J. Energy Chem. 32 (2019) 57–62.
- [28] C. Zhao, Y. Li, Z. He, Y. Jiang, L. Li, F. Jiang, H. Zhou, J. Zhu, W. Meng, L. Wang, L. Dai, J. Energy Chem. 29 (2019) 103–110.
- [29] L. Cao, M. Skyllas-Kazacos, C. Menictas, J. Noack, J. Energy Chem. 27 (2018) 1269–1291.
- [30] M. Ulaganathan, V. Aravindan, Q. Yan, S. Madhavi, M. Skyllas-Kazacos, T.M. Lim, Adv. Mater. Interfaces 3 (2016) 1500309.
- [31] L. Wei, T.S. Zhao, G. Zhao, L. An, L. Zeng, Appl. Energy 176 (2016) 74–79.
- [32] L. Yue, W. Li, F. Sun, L. Zhao, L. Xing, Carbon 48 (2010) 3079–3090.
- [33] M.E. Lee, H.J. Jin, Y.S. Yun, RSC Adv. 7 (2017) 43227–43232.
- [34] Z. Liu, B. Wang, L. Yu, J. Energy Chem. 27 (2018) 1369–1375.
- [35] M. Park, J. Ryu, Y. Kim, J. Cho, Energy Environ. Sci. 7 (2014) 3727–3735.
- [36] M.M. Mohideen, Y. Liu, S. Ramakrishna, Appl. Energy 257 (2020) 114027–114035.
- [37] Z. Gonzalez, C. Botas, P. Alvarez, S. Roldan, C. Blanco, R. Santamaría, M. Granda, R. Menendez, Carbon 50 (2012) 828–834.
- [38] H. Jiang, W. Shyy, L. Zeng, R. Zhang, T. Zhao, J. Mater. Chem. A 6 (2018) 13244–13253.
- [39] X.L. Chen, W.S. Li, C.L. Tan, W. Li, Y.Z. Wu, J. Power Sources 184 (2008) 668–674.
- [40] Y. Jiang, G. Cheng, Z. He, J. Chen, Y. Li, J. Zhu, W. Meng, H. Zhou, L. Dai, L. Wang, J. Electrochem. Soc. 166 (2019) 3918–3926.
- [41] D. Cheng, M. Tian, B. Wang, J. Zhang, J. Chen, X. Feng, Z. He, L. Dai, L. Wang, J. Colloid Interface Sci. 572 (2020) 216–226.
- [42] Y.R. Lv, Y.H. Li, C. Han, J.F. Chen, Z.X. He, J. Zhu, L. Dai, W. Meng, L. Wang, J. Colloid Interface Sci. 566 (2020) 434–443.
- [43] Z. Jia, B. Wang, A. Feng, J. Liu, C. Zhang, M. Zhang, G. Wu, Ceram. Int. 45 (2019) 15854–15859.
- [44] G. Mills, M.S. Gordon, H. Metiu, J. Chem. Phys. 118 (2003) 4198–4205.
- [45] L. Yang, L. Qian, X. Tian, J. Li, J. Dai, Y. Guo, D. Xiao, Chem. Asian J. 9 (2014) 1579–1585.
- [46] E. Agar, C.R. Dennison, K.W. Knehr, E.C. Kumbur, J. Power Sources 225 (2013) 89–94.
- [47] A.M. Pezeshki, J.T. Clement, G.M. Veith, T.A. Zawodzinski, M.M. Mench, J. Power Sources 294 (2015) 333–338.
- [48] K.J. Kim, S.W. Lee, T. Yim, J.G. Kim, J.W. Choi, J.H. Kim, M.S. Park, Y.J. Kim, Sci. Rep. 4 (2014) 6906.
- [49] Y. Lu, W. Li, F. Sun, L. Zhao, L. Xing, Carbon 48 (2010) 3079–3090.
- [50] W. Zhang, J. Xi, Z. Li, H. Zhou, L. Liu, Z. Wu, X. Qiu, Electrochim. Acta 89 (2013) 429–435.
- [51] Z. Gonzalez, A. Sanchez, C. Blanco, M. Granda, R. Menendez, R. Santamaría, Electrochim. Commun. 13 (2011) 1379–1382.
- [52] M. Park, Y.J. Jung, J. Kim, H.I. Lee, J. Cho, Nano Lett. 13 (2013) 4833–4839.
- [53] J. Maruyama, S. Maruyama, T. Fukuhara, K. Hanafusa, J. Phys. Chem. C 121 (2017) 24425–24433.
- [54] D. Cheng, Y. Li, J. Zhang, M. Tian, B. Wang, Z. He, L. Dai, L. Wang, Carbon 170 (2020) 527–542.
- [55] M. Rychcik, M. Skyllas-Kazacos, J. Power Sources 19 (1987) 45–54.
- [56] V. Mahanta, M. Raju, R. Kothandaraman, Mater. Lett. 247 (2019) 63–66.
- [57] D.S. Yang, J.H. Han, J.W. Jeon, J.Y. Lee, D.G. Kim, D.H. Seo, B.G. Kim, T.H. Kim, Y.T. Hong, Mater. Today Energy 11 (2019) 159–165.
- [58] Y. Xiang, W.A. Daoud, J. Mater. Chem. A 7 (2019) 5589–5600.
- [59] L. Wu, Y. Shen, L. Yu, J. Xi, X. Qiu, Nano Energy 28 (2016) 19–28.
- [60] L. Yu, F. Un, W. Xiao, L. Xu, J. Xi, Chem. Eng. J. 356 (2019) 622–631.
- [61] Z.X. He, G. Cheng, Y.Q. Jiang, Y.H. Li, J. Zhu, W. Meng, H.Z. Zhou, L. Dai, L. Wang, Int. J. Hydrogen Energy 45 (2020) 3959–3970.
- [62] R.H. Huang, C.H. Sun, T.M. Tseng, W.K. Chao, K.L. Hsueh, F.S. Shieh, J. Electrochim. Soc. 159 (2012) 1579–1586.
- [63] S. Jeong, S. Kim, Y. Kwon, Electrochim. Acta 114 (2013) 439–447.
- [64] T.M. Tseng, R.H. Huang, C.Y. Huang, K.L. Hsueh, F.S. Shieh, J. Electrochim. Soc. 160 (2013) 690–696.
- [65] W.H. Wang, X.D. Wang, Electrochim. Acta 52 (2007) 6755–6762.
- [66] H. Zhou, H. Zhang, P. Zhao, B. Yi, Electrochim. Acta 51 (2006) 6304–6312.
- [67] H.M. Tsai, S.J. Yang, C.C.M. Ma, X. Xie, Electrochim. Acta 77 (2012) 232–236.
- [68] C.H. Chang, T.S. Yuen, Y. Nagao, H. Yugami, J. Power Sources 195 (2010) 5938–5941.
- [69] C.P.D. Leon, A. Frias-Ferrer, J. Gonzalez-Garcia, D.A. Szanto, F.C. Walsh, J. Power Sources 160 (2006) 716–732.
- [70] D. Cheng, Y. Li, C. Han, Z. He, J. Zhu, L. Dai, W. Meng, L. Wang, Colloids Surf. A 586 (2020) 124137–124145.
- [71] S.Y. Huang, P. Ganeshan, H.Y. Jung, B.N. Popov, J. Power Sources 198 (2012) 23–29.
- [72] B. Li, M. Gu, Z. Nie, Y. Shao, Q. Luo, X. Wei, X. Li, J. Xiao, C. Wang, V. Sprenkle, Nano Lett. 13 (2013) 1330–1335.
- [73] D.J. Suarez, Z. Gonzalez, C. Blanco, M. Granda, R. Menendez, R. Santamaría, ChemSusChem 7 (2014) 914–918.
- [74] X. Yang, T. Liu, C. Xu, H. Zhang, H. Zhang, J. Energy Chem. 26 (2017) 1–7.
- [75] H.R. Jiang, Y.K. Zeng, M.C. Wu, W. Shyy, T.S. Zhao, Appl. Energy 240 (2019) 226–235.
- [76] L. Wei, T.S. Zhao, L. Zeng, X.L. Zhou, Y.K. Zeng, Appl. Energy 180 (2016) 386–391.
- [77] J. Shen, S. Liu, Z. He, L. Shi, Electrochim. Acta 151 (2015) 297–305.
- [78] Y. Lv, J. Zhang, Z. Lv, C. Wu, Y. Liu, H. Wang, S. Lu, Y. Xiang, Electrochim. Acta 253 (2017) 78–84.
- [79] T. Liu, X. Li, H. Nie, C. Xu, H. Zhang, J. Power Sources 286 (2015) 73–81.
- [80] P. Leung, J. Palma, E. Garcia-Quismondo, L. Sanz, M.R. Mohamed, M. Anderson, J. Power Sources 310 (2016) 1–11.
- [81] S. Mehbobah, A. Mehmood, J.Y. Lee, H.J. Shin, J. Hwang, S. Abbas, H.Y. Ha, J. Mater. Chem. A 5 (2017) 17388–17400.
- [82] H. Zhou, J. Xi, Z. Li, Z. Zhang, L. Yu, L. Liu, X. Qiu, L. Chen, RSC Adv. 4 (2014) 61912–61918.
- [83] M. Jing, X. Zhang, X. Fan, L. Zhao, C. Yan, Electrochim. Acta 215 (2016) 57–65.
- [84] Z. Lin, L. Lan, P. Xiao, S. Sun, Y. Li, W. Song, P. Gao, L. Wang, H. Ning, J. Peng, Appl. Phys. Lett. 107 (2015) 112108.
- [85] A. Fetyan, G.A. El Nagar, I. Derr, P. Kubella, H. Dau, C. Roth, Electrochim. Acta 268 (2018) 59–65.
- [86] W. Yang, Y.L. Qi, Y.J. Ma, X. Li, X.J. Guo, J.Z. Gao, M. Chen, Mater. Chem. Phys. 84 (2004) 52–57.
- [87] B.H. Lee, S. Park, M. Kim, A.K. Sinha, S.C. Lee, E. Jung, W.J. Chang, K.S. Lee, J.H. Kim, S.P. Cho, H. Kim, K.T. Nam, T. Hyeon, Nat. Mater. 18 (2019) 620–628.
- [88] S. Zhao, J. Chen, Y. Liu, Y. Jiang, C. Jiang, Z. Yin, Y. Xiao, S. Cao, Chem. Eng. J. 367 (2019) 249–259.
- [89] X. Jia, X. Zhang, N. Rui, X. Hu, C.J. Liu, Appl. Catal. B 244 (2019) 159–169.
- [90] W. Li, X. Nie, X. Jiang, A. Zhang, F. Ding, M. Liu, Z. Liu, X. Guo, C. Song, Appl. Catal. B 220 (2018) 397–408.
- [91] J. Ye, X. Zhao, Y. Ma, J. Su, C. Xiang, K. Zhao, M. Ding, C. Jia, L. Sun, Adv. Energy Mater. 10 (2020), 1904041.
- [92] J. Ryu, W. Choi, Environ. Sci. Technol. 42 (2008) 294–300.
- [93] T. Tran, K. McCormac, J. Li, Z. Bi, J. Wu, Electrochim. Acta 117 (2014) 68–75.

- [94] J. Vazquez-Galvan, C. Flox, C. Fabrega, E. Ventosa, A. Parra, T. Andreu, J.R. Morante, *ChemSusChem* 10 (2017) 2089–2098.
- [95] J. Vazquez-Galvan, C. Flox, J.R. Jervis, A.B. Jorge, P.R. Shearing, J.R. Morante, *Carbon* 148 (2019) 91–104.
- [96] Z.X. He, M.M. Li, Y.H. Li, J. Zhu, Y.Q. Jiang, W. Meng, H.Z. Zhou, L. Wang, L. Dai, *Electrochim. Acta* 281 (2018) 601–610.
- [97] D.X. Cheng, G. Cheng, Z.X. He, L. Dai, L. Wang, *Int. J. Energy Res.* 43 (2019) 4473–4482.
- [98] A.W. Bayeh, D.M. Kabtamu, Y.C. Chang, G.C. Chen, H.Y. Chen, G.Y. Lin, T.R. Liu, T.H. Wondimu, K.C. Wang, C.H. Wang, *J. Mater. Chem. A* 6 (2018) 13908–13917.
- [99] J. Lin, C. Ma, Q. Wang, Y. Xu, G. Ma, J. Wang, H. Wang, C. Dong, C. Zhang, M. Ding, *Appl. Catal. B* 243 (2019) 262–272.
- [100] H. Zhou, Y. Shen, J. Xi, X. Qiu, L. Chen, *ACS Appl. Mater. Interfaces* 8 (2016) 15369–15378.
- [101] Z.X. He, M.M. Li, Y.H. Li, C.C. Li, Z. Yi, J. Zhu, L. Dai, W. Meng, H.Z. Zhou, L. Wang, *Electrochim. Acta* 309 (2019) 166–176.
- [102] A.W. Bayeh, D.M. Kabtamu, Y.C. Chang, G.C. Chen, H.Y. Chen, G.Y. Lin, T.R. Liu, T.H. Wondimu, K.C. Wang, C.H. Wang, *ACS Sustainable Chem. Eng.* 6 (2018) 3019–3028.
- [103] B. Li, M. Gu, Z. Nie, X. Wei, C. Wang, V. Sprenkle, W. Wang, *Nano Lett.* 14 (2014) 158–165.
- [104] C. Yao, H. Zhang, T. Liu, X. Li, Z. Liu, *J. Power Sources* 218 (2012) 455–461.
- [105] D.M. Kabtamu, J.Y. Yu, Y.C. Chang, C.H. Wang, *J. Mater. Chem. A* 4 (2016) 11472–11480.
- [106] D.M. Kabtamu, Y.C. Chang, G.Y. Lin, A.W. Bayeh, J.Y. Chen, T.H. Wondimu, C.H. Wang, *Sustain. Energy Fuels* 1 (2017) 2091–2100.
- [107] M.G. Hosseini, S. Mousavihashemi, S. Murcia-Lopez, C. Flox, T. Andreu, J.R. Morante, *Carbon* 136 (2018) 444–453.
- [108] Y. Xiang, W.A. Daoud, *Electrochim. Acta* 290 (2018) 176–184.
- [109] P. Hien Thi Thu, C. Jo, J. Lee, Y. Kwon, *RSC Adv.* 6 (2016) 17574–17582.
- [110] L. Cao, M. Skyllas-Kazacos, D.W. Wang, *ChemElectroChem* 4 (2017) 1836–1839.
- [111] Y. Shen, H. Xu, P. Xu, X. Wu, Y. Dong, L. Lu, *Electrochim. Acta* 132 (2014) 37–41.
- [112] G. Hai, J. Huang, L. Cao, Y. Jie, J. Li, X. Wang, G. Zhang, *J. Alloys. Compd.* 690 (2017) 239–248.
- [113] L. Xiao, S. Zhang, J. Huang, *Power Technol.* 258 (2014) 297–303.
- [114] A.W. Bayeh, D.M. Kabtamu, Y.C. Chang, G.C. Chen, H.Y. Chen, T.R. Liu, T.H. Wondimu, K.C. Wang, C.H. Wang, *ACS Appl. Energy Mater.* 2 (2019) 2541–2551.
- [115] G. Yang, X. Li, T. Chen, W. Gao, Y. Dai, X. Li, *J. Nanosci. Nanotechnol.* 20 (2020) 4203–4209.
- [116] C. Ma, R. Sun, Y. Chen, J. Sun, H. Ji, Y. Li, G. Yang, *J. Mater. Sci.* 55 (2020) 5545–5553.
- [117] K.J. Kim, M.S. Park, J.H. Kim, U. Hwang, N.J. Lee, G. Jeong, Y.J. Kim, *Chem. Commun.* 48 (2012) 5455–5457.
- [118] L. Zeng, T.S. Zhao, L. Wei, Y.K. Zeng, X.L. Zhou, *Energy Technol.* 6 (2018) 1228–1236.
- [119] A.D. Blasi, C. Busaccaa, O. Di Blas, N. Briguglio, G. Squadrato, V. Antonuccia, *Appl. Energy* 190 (2017) 165–171.
- [120] Z. He, L. Dai, S. Liu, L. Wang, C. Li, *Electrochim. Acta* 176 (2015) 1434–1440.
- [121] Y. Ji, J.L. Li, S.F.Y. Li, *J. Mater. Chem. A* 5 (2017) 15154–15166.
- [122] A. Ejigu, M. Edwards, D.A. Walsh, *ACS Catal.* 5 (2015) 7122–7130.
- [123] Q. Ma, Q. Deng, H. Sheng, W. Ling, H.R. Wang, H.W. Jiao, X.W. Wu, W.X. Zhou, X.X. Zeng, Y.X. Yin, Y.G. Guo, *Sci. China Chem.* 61 (2018) 732–738.
- [124] Y. Jiang, X. Feng, G. Cheng, Y. Li, C. Li, Z. He, J. Zhu, W. Meng, H. Zhou, L. Dai, L. Wang, *Electrochim. Acta* 322 (2019) 134754–134762.
- [125] Y. Xiang, W.A. Daoud, *J. Power Sources* 416 (2019) 175–183.
- [126] N. Yun, J.J. Park, O.O. Park, K.B. Lee, J.H. Yang, *Electrochim. Acta* 278 (2018) 226–235.
- [127] J.J. Park, J.H. Park, O.O. Park, J.H. Yang, *Carbon* 110 (2016) 17–26.
- [128] F. Gobal, M. Faraji, *RSC Adv.* 5 (2015) 68378–68384.
- [129] X. Wu, H. Xu, L. Lu, H. Zhao, J. Fu, Y. Shen, P. Xu, Y. Dong, *J. Power Sources* 250 (2014) 274–278.
- [130] J.H. Kim, A. Mirzaei, H.W. Kim, S.S. Kim, *Sens. Actuators B* 285 (2019) 358–367.
- [131] C. Wang, F. Lan, Z. He, X. Xie, Y. Zhao, H. Hou, L. Guo, V. Murugadoss, H. Liu, Q. Shao, Q. Gao, T. Ding, R. Wei, Z. Guo, *ChemSusChem* 12 (2019) 1576–1590.
- [132] S. Zinatloo-Ajabshir, M.S. Morassaei, M. Salavati-Niasari, *J. Environ. Manage.* 233 (2019) 107–119.
- [133] S. Mehboob, G. Ali, H.J. Shin, J. Hwang, S. Abbas, K.Y. Chung, H.Y. Ha, *Appl. Energy* 229 (2018) 910–921.
- [134] J. Maruyama, S. Maruyama, T. Fukuhara, T. Nagaoka, K. Hanafusa, J. Beilstein, *Nanotechnol.* 10 (2019) 985–992.
- [135] X. He, Z. He, Q. Zou, L. Wu, *Int. J. Energy Res.* 44 (2020) 2100–2109.
- [136] R. Zhang, K. Li, S. Ren, J. Chen, X. Feng, Y. Jiang, Z. He, L. Dai, L. Wang, *Appl. Surf. Sci.* 526 (2020) 146685–146695.